



ІНСТИТУТ
ФІЗИКИ
КОНДЕНСОВАНИХ
СИСТЕМ

ICMP-99-25E

I.V.Stasyuk, R.R.Levitskii, I.R.Zachek, A.P.Moina, A.S.Duda

INFLUENCE OF SHEAR STRESS σ_6 ON THE PHASE
TRANSITION AND PHYSICAL PROPERTIES OF KD_2PO_4 TYPE
FERROELECTRICS

PACS: 77.80.Bh, 77.84.Fa

УДК: 533, 536

Вплив напруги зсуву σ_6 на фазовий перехід і фізичні властивості сегнетоелектриків типу KD_2PO_4

І.В.Стасюк, Р.Р.Левицький, І.Р.Зачек, А.П. Моїна, А.С.Дуда

Анотація. В наближенні чотиричастинкового кластера в рамках моделі протонного впорядкування досліджується вплив зсувної напруги σ_6 на фазовий перехід, статичні діелектричні, пружні, п'єзоелектричні та теплові властивості дейтерованих сегнетоелектриків типу KD_2PO_4 . Розраховано термодинамічні потенціали та фізичні характеристики кристалів при наявності напруги σ_6 . Проведено числовий аналіз отриманих результатів; знайдено набір значень параметрів теорії, які забезпечують задовільний опис наявних експериментальних даних. Побудовано $T_C - \sigma_6$ фазову діаграму; досліджено температурні, вказано на можливі баричні залежності розрахованих величин. Показано, що вплив напруги σ_6 аналогічний до дії зовнішнього поля, спряженого до параметра порядку.

Influence of shear stress σ_6 on the phase transition and physical properties of KD_2PO_4 type ferroelectrics.

I.V.Stasyuk, R.R.Levitskii, I.R.Zachek, A.P.Moina, A.S.Duda

Abstract. Within the four-particle cluster approximation for the proton ordering model we study the influence of shear stress σ_6 on the phase transition, static dielectric, elastic and thermal properties of deuterated KD_2PO_4 type ferroelectrics. Thermodynamic potentials and physical characteristics of the crystals in the presence of stress σ_6 are calculated. Numerical analysis of the obtained results is performed, and the set of the theory parameters providing the best fit to the available experimental data is found. The $T_C - \sigma_6$ phase diagram is constructed; temperature dependences of the calculated quantities are studied, possible stress dependences are indicated. Influence of σ_6 stress is analogous to that of electric field conjugate to the order parameter.

Подается в Condensed Matter Physics
Submitted to Condensed Matter Physics

1. Introduction

More than sixty years have passed since the discovery of the ferroelectricity in the KH_2PO_4 crystals. During those years, a huge number of papers has been devoted to the studies of the phase transitions in the crystals of the KH_2PO_4 family and of their physical properties. The most prominent peculiarity of these studies is a strong connection between theory and experiment, which is thought to be an important source of the obtained progress in microscopic understanding of their properties. In this aspect, the high pressure studies of these crystals come extremely important. External pressure changes the internal structure of the system, altering thereby the molecular potentials in the crystal and its dielectric and thermal properties. And shear stresses give rise to shear piezoelectric lattice strains induced also by external electric fields via the piezoelectric effect; that allows one to consistently explore the electric, electromechanic and thermal characteristics of the crystals.

A microscopic model of strained KH_2PO_4 type crystals has been proposed in [1–3]. According to this model, external mechanical stresses give rise to additional internal fields, linear in strains and (in the case of diagonal components of stress tensor) mean values of quasispins. Influence of stresses of different symmetries on energies of deuteron configurations was studied.

In [1–3] there were also explored the effects of $\sigma_{12} = \sigma_{xx} - \sigma_{yy}$ stress on the transition temperature to the ferroelectric phase and the relations between the applied stress $\sigma_{xx} - \sigma_{yy}$ and the induced strain $\varepsilon_{12} = \varepsilon_{xx} - \varepsilon_{yy}$ taking into account the deuteron rearrangement on hydrogen bonds. In [4,5] using the model proposed in [1–3], within the cluster approximation taking into account the short-range and long-range interactions and stress σ_{12} , the dielectric, piezoelectric, and thermal characteristics of KD_2PO_4 were calculated and studied. It has been shown that the stress σ_{12} can lead to a phase transition to the monoclinic phase.

Influence of hydrostatic pressure and uniaxial pressure $-p = \sigma_3$ on the physical properties of the KD_2PO_4 type crystals was investigated in [6–8]. We showed that under the proper choice of the theory parameters, a satisfactory description of the experimental data for the pressure dependences of spontaneous polarization, longitudinal static dielectric permittivity and transition temperature was obtained. Using the Glauber model [9] the expressions for the real and imaginary parts of the longitudinal dynamic dielectric permittivity of KD_2PO_4 were found, and their temperature and frequency dependences at different values of hydrostatic pressure were calculated.

It is also interesting to study the influence of the shear stress σ_6 giving rise to a shear strain $\varepsilon_6 = \varepsilon_{xy}$, which transforms after the irreducible representation B_2 . After this representation, polarization P_3 transforms too; hence, the influence of external stress $\sigma_6 = \sigma_{xy}$ is similar to that of electric field E_3 . Importance of this study results also from the fact that spontaneous polarization P_3 in KD_2PO_4 is accompanied by spontaneous shear strain ε_6 .

In [10] the dielectric, piezoelectric, and elastic properties of KH_2PO_4 with taking into account the strain ε_6 induced by the piezoelectric effect are studied within the modified Slater model.

Experimental measurements of dielectric, electromechanic, and elastic characteristics of $\text{K}(\text{H}_{1-x}\text{D}_x)_2\text{PO}_4$ were performed in several works. Thus, in [15] the temperature dependences of the dielectric permittivities of free and clamped KH_2PO_4 crystal, piezoelectric constants d_{36} , e_{36} , h_{36} and elastic constants c_{66}^P , c_{66}^E and s_{66}^P , s_{66}^E were reported. Temperature dependences of the piezoelectric module d_{36} of the KH_2PO_4 crystal at direct and inverse piezoelectric effect are given in [16] and [17], respectively. Temperature dependence of elastic constant c_{66}^E for KH_2PO_4 is presented in [18]. Experimental data for the temperature dependence of d_{36} , ε_{33} and s_{66}^E for a partially deuterated crystal with $x = 0.89$ are given in [19,20].

In this paper we study the influence of the shear stress σ_6 on the phase transition and physical properties of deuterated ferroelectric crystals of the KH_2PO_4 family. We shall also compare the obtained results for thermodynamic, dielectric, elastic, and piezoelectric characteristics of the crystals with the corresponding experimental data.

2. The crystal Hamiltonian

We consider a system of deuterons moving on O–D–...–O bonds in deuterated crystals of the KD_2PO_4 type. The primitive cell of such a crystal is composed of two neighbouring PO_4 tetrahedra together with four hydrogen bonds attached to one of them ("A" type tetrahedra). Hydrogen bonds going to another ("B" type) tetrahedron belong to four nearest structural elements surrounding it (see the figure below).

Hamiltonian of a deuteron subsystem of the KD_2PO_4 type crystals taking into account the short-range and long-range interactions in the presence of the shear stress $\sigma_6 = \sigma_{xy}$ giving rise to the strain $\varepsilon_6 = \varepsilon_{xy}$ and of the external electric fields E_i ($i = 1, 2, 3$) applied along the

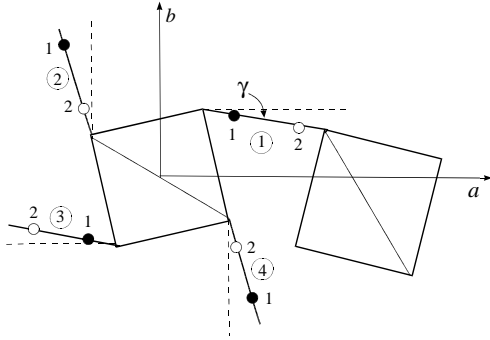


Figure 1. Primitive cell of the KD_2PO_4 crystal. Numbers in circles correspond to hydrogen bonds; 1,2 are the deuteron equilibrium sites. By dashed lines we show the directions of hydrogen bonds in an unstrained crystal in the paraelectric phase. a , b are the axes of an undeformed $I\bar{4}2d$ cell; γ is an angle between the directions of hydrogen bonds in strained and unstrained crystals.

crystallographic axes (a, b, c) reads

$$\hat{H}_i = \frac{\bar{v}N}{2} c_{66}^{E_0} \varepsilon_6^2 - \bar{v}N e_{36}^0 E_3 \varepsilon_6 - \frac{\bar{v}N}{2} \chi_{ii}^0 E_i^2 + \sum_{q'f'qf} J_{ff'}(qq') \frac{\langle \sigma_{qf} \rangle}{2} \frac{\langle \sigma_{q'f'} \rangle}{2} - \sum_{qf} [2\mu F_f^z(6) + \mu_{fi} E_i] \frac{\sigma_{qf}}{2} + \hat{H}_{\text{short}}. \quad (2.1)$$

The first term in the right hand side of (2.1) corresponds to that part of the elastic energy which does not depend on hydrogen arrangement ($c_{66}^{E_0}$ is the so called “seed” elastic constant); the second term in (2.1) is the energy of interaction between polarization induced by the piezoelectric effect due to the strain ε_6 (not taking into account the hydrogen subsystem contribution) and field E_3 (e_{36}^0 is the seed coefficient of the piezoelectric stress); the third term is the energy due to polarization induced by external field independently of the hydrogen configuration (χ_{33}^0 is the seed dielectric susceptibility). The last term in (2.1) describes the short range configurational interactions between deuterons around the “A” and “B” type tetrahedra. Two eigenvalues of Ising spin $\sigma_{qf} = \pm 1$ are assigned to two equilibrium positions of a deuteron on the f -th bond in the q -th unit cell ($\sigma_{qf} = \pm 1$). $\bar{v} = v/k_B$, v is the primitive cell volume; k_B is the Boltzmann constant. F_f^i are internal fields, arising in strained crystals, which include the effective long-range interaction be-

tween deuterons (taken into account in the mean field approximation) and the additional internal fields related to the strain ε_6 [3]:

$$\begin{aligned} 2\mu F^z(6) &= 2\mu F_1^z(6) = -2\mu F_2^z(6) = -2\mu F_3^z(6) = 2\mu F_4^z(6) = \\ &= 2\nu_c \eta^{(1)z}(6) - 2\psi_6 \varepsilon_6, \\ 2\mu F_1^{xy}(6) &= 2\nu_1 \eta_1^{(1)xy}(6) + 2\nu_3 \eta_3^{(1)xy}(6) + \\ &+ 2\nu_2 [\eta_2^{(1)xy}(6) + \eta_4^{(1)xy}(6)] - 2\psi_6 \varepsilon_6, \\ 2\mu F_2^{xy}(6) &= 2\nu_2 [\eta_1^{(1)xy}(6) + \eta_3^{(1)xy}(6)] + \\ &+ 2\nu_1 \eta_2^{(1)xy}(6) + 2\nu_3 \eta_4^{(1)xy}(6) - 2\psi_6 \varepsilon_6, \\ 2\mu F_3^{xy}(6) &= 2\nu_3 \eta_1^{(1)xy}(6) + 2\nu_1 \eta_3^{(1)xy}(6) + \\ &+ 2\nu_2 [\eta_2^{(1)xy}(6) + \eta_4^{(1)xy}(6)] - 2\psi_6 \varepsilon_6, \\ 2\mu F_4^{xy}(6) &= 2\nu_2 [\eta_1^{(1)xy}(6) + \eta_3^{(1)xy}(6)] + \\ &+ 2\nu_3 \eta_2^{(1)xy}(6) + 2\nu_1 \eta_4^{(1)xy}(6) - 2\psi_6 \varepsilon_6, \end{aligned} \quad (2.2)$$

where

$$\eta^{(1)z}(6) = \langle \sigma_{q1} \rangle^z = \langle \sigma_{q2} \rangle^z = \langle \sigma_{q3} \rangle^z = \langle \sigma_{q4} \rangle^z, \quad \eta_f^{(1)xy}(6) = \langle \sigma_{qf} \rangle^{xy};$$

$$\nu_c = \nu_1 + 2\nu_2 + \nu_3; \quad \nu_1 = \frac{J_{11}}{4}, \nu_2 = \frac{J_{12}}{4}, \nu_3 = \frac{J_{13}}{4};$$

$J_{ff'} = \sum_{\mathbf{R}_q - \mathbf{R}_{q'}} J_{ff'}(qq')$ is the Fourier transform of the long-range deuteron-deuteron interaction, ψ_6 is the so called deformation potential; $\mu = e\delta$ is the dipole moment of a hydrogen bond; δ is the D-site distance.

In (2.1) and (2.2) we do not take into account piezoelectric shear strains ε_4 or ε_5 induced by electric fields E_1 and E_2 , respectively.

The Hamiltonian is usually chosen such that to reproduce the energy levels of the Slater-type model for KDP (see, for instance [11]) – the Slater energies ε , w , and w_1 ($\varepsilon \ll w \ll w_1$), determined by the energies of up-down ε_s , lateral ε_a , single-ionized ε_1 , and double-ionized ε_0 deuteron configurations.

$$\varepsilon = \varepsilon_a - \varepsilon_s, \quad w = \varepsilon_1 - \varepsilon_s, \quad w_1 = \varepsilon_0 - \varepsilon_s.$$

If $\varepsilon_6 = 0$, configurations with two hydrogens in potential wells being close to upper and lower oxygens of a given PO_4 group (each PO_4 tetrahedron is oriented such that two of its edges are parallel to the ab plane) and with the hydrogens on the two other bonds being close to the neighboring tetrahedra, have the same energy ε_s , assumed to be the lowest. Correspondingly, lateral configurations with two hydrogens close to an

upper and a lower oxygens are four-fold degenerated; single-ionized with only one (or three) hydrogens close to a given group are eight-fold degenerated, and double-ionized with four hydrogens (or without any) are twice degenerated.

However, the strain σ_6 splits certain deuteron configurations of the conventional Slater-Takagi model. In Table below we present all possible deuteron configurations and their energies. Since the system is not any longer symmetric with respect to a reflection in the ab plane σ_h or to the reflection with $\pi/4$ rotation around the c -axis S_4 (both operations change the sign of polarization and strain ε_6), the up-down configurations ($i = 1, 2$) split to two different levels, and lateral configurations split to two groups of twice degenerated levels each ($i = 5, 6$) and ($i = 7, 8$). Configurations within each group are symmetric with respect to $\pi/2$ rotation C_2 . Similarly, single-ionized configuration are divided into two groups, within each the c -component of dipole moments assigned to a configuration are directed up ($i = 9, 10, 11, 12$) or down ($i = 13, 14, 15, 16$).

Here we assume that the strain ε_6 alters the energies of deuteron configurations only by splitting the degenerated levels due to lowering of the system symmetry. From geometric point of view, this happens mostly because the angle between perpendicular in the paraelectric phase hydrogen bonds is changed, whereas in the hydrostatic pressure case the changes are usually attributed to pressure-induced changes in the D-site distance δ [6,12].

To rewrite the energies of deuteron configurations E_{i6} in terms of pseudospins, we associate the configuration operator \hat{N}_i with the configuration i according to the following rule: each operator is a product of four factors, one per each hydrogen bond, each factor being equal to $\frac{1}{2}(1 + \sigma_{qf})$ if deuteron is in the first minimum at the f -th bond and $\frac{1}{2}(1 - \sigma_{qf})$ otherwise. Then the Hamiltonian of the short-range interactions takes the form

$$\begin{aligned} \hat{H}_{\text{short}}(6) &= \sum_{q=1}^N \sum_{i=1}^{16} [\hat{N}_i^A(q) + \hat{N}_i^B(q)] = \quad (2.3) \\ &= \sum_{q=1}^N \left\{ \frac{\varepsilon_6}{4} (-\delta_{s6} + 2\delta_{16}) \sum_{f=1}^4 \frac{\sigma_{qf}}{2} + \right. \\ &- \varepsilon_6 (\delta_{s6} + 2\delta_{16}) \left[\frac{\sigma_{q1}}{2} \frac{\sigma_{q2}}{2} \frac{\sigma_{q3}}{2} + \frac{\sigma_{q1}}{2} \frac{\sigma_{q2}}{2} \frac{\sigma_{q4}}{2} + \frac{\sigma_{q1}}{2} \frac{\sigma_{q3}}{2} \frac{\sigma_{q4}}{2} + \frac{\sigma_{q2}}{2} \frac{\sigma_{q3}}{2} \frac{\sigma_{q4}}{2} \right] + \\ &+ (V + \delta_6 \varepsilon_6) \left[\frac{\sigma_{q1}}{2} \frac{\sigma_{q2}}{2} + \frac{\sigma_{q3}}{2} \frac{\sigma_{q4}}{2} \right] + (V - \delta_6 \varepsilon_6) \left[\frac{\sigma_{q2}}{2} \frac{\sigma_{q3}}{2} + \frac{\sigma_{q4}}{2} \frac{\sigma_{q1}}{2} \right] + \end{aligned}$$

i		E_{i6}	i		E_{i6}		
1		$++++$	$\varepsilon_s - \delta_{s6}\varepsilon_6$	9		$----+$	$\varepsilon_1 - \delta_{16}\varepsilon_6$
2		$----$	$\varepsilon_s + \delta_{s6}\varepsilon_6$	10		$---+$	
3		$+--+$	ε_0	11		$-+--$	
4		$-+-+$	ε_0	12		$+---$	
5		$++--$	$\varepsilon_a + \delta_{a6}\varepsilon_6$	13		$++--$	$\varepsilon_1 + \delta_{16}\varepsilon_6$
6		$--++$	$\varepsilon_a + \delta_{a6}\varepsilon_6$	14		$++--$	
7		$+++-$	$\varepsilon_a - \delta_{a6}\varepsilon_6$	15		$-+++$	
8		$+--+$	$\varepsilon_a - \delta_{a6}\varepsilon_6$	16		$-+++$	

$$+ U \left[\frac{\sigma_{q1} \sigma_{q3}}{2} + \frac{\sigma_{q2} \sigma_{q4}}{2} \right] + \Phi \frac{\sigma_{q1} \sigma_{q2} \sigma_{q3} \sigma_{q4}}{2} + \sum_{q=1}^N \sum_{i=1}^{16} \hat{N}_i^B(q).$$

Here the following notations are used

$$\begin{aligned} V &= V_{12} = V_{23} = V_{34} = V_{41} = -\frac{1}{2}w_1, \\ U &= V_{13} = V_{24} = \frac{1}{2}w_1 - \varepsilon, \quad \Phi = 4\varepsilon + 2w_1 - 8w, \\ \varepsilon &= \varepsilon_a - \varepsilon_s, \quad w = \varepsilon_1 - \varepsilon_s, \quad w_1 = \varepsilon_0 - \varepsilon_s, \end{aligned}$$

where $\varepsilon_s, \varepsilon_a, \varepsilon_1, \varepsilon_0$ are energies of up-down, lateral, single-ionized and double-ionized deuteron configurations in an unstrained crystal, respectively.

The further calculations will be performed in the four-particle cluster approximation. The cluster Hamiltonian in the presence of the stress σ_6 and electric field E_i reads

$$\begin{aligned} \hat{H}_{q4}^{iA}(6) &= \frac{e}{4}(-\delta_{s6} + 2\delta_{16}) \sum_{f=1}^4 \frac{\sigma_{qf}}{2} + \\ & -\varepsilon_6(\delta_{s6} + 2\delta_{16}) \left[\frac{\sigma_{q1} \sigma_{q2} \sigma_{q3}}{2} + \frac{\sigma_{q1} \sigma_{q2} \sigma_{q4}}{2} + \frac{\sigma_{q1} \sigma_{q3} \sigma_{q4}}{2} + \frac{\sigma_{q2} \sigma_{q3} \sigma_{q4}}{2} \right] + \\ & + (V + \delta_6 \varepsilon_6) \left[\frac{\sigma_{q1} \sigma_{q2}}{2} + \frac{\sigma_{q3} \sigma_{q4}}{2} \right] + (V - \delta_6 \varepsilon_6) \left[\frac{\sigma_{q2} \sigma_{q3}}{2} + \frac{\sigma_{q4} \sigma_{q1}}{2} \right] + \\ & + U \left[\frac{\sigma_{q1} \sigma_{q3}}{2} + \frac{\sigma_{q2} \sigma_{q4}}{2} \right] + \Phi \frac{\sigma_{q1} \sigma_{q2} \sigma_{q3} \sigma_{q4}}{2} - \sum_f \frac{z_{f6}^i \sigma_{qf}}{\beta}. \end{aligned} \quad (2.4)$$

In (2.4)

$$\begin{aligned} z_6^z &= z_{16}^z = z_{26}^z = z_{36}^z = z_{46}^z = \beta[-\Delta_6^z + 2\mu F^z(6) + \mu_3 E_3]; \\ z_{16}^x &= \beta[-\Delta_6^x + 2\mu F_1^x(6) + \mu_\perp \cos \gamma E_1], \\ z_{26}^x &= \beta[-\Delta_6^x + 2\mu F_2^x(6) - \mu_\perp \sin \gamma E_1], \\ z_{36}^x &= \beta[-\Delta_6^x + 2\mu F_3^x(6) - \mu_\perp \cos \gamma E_1], \\ z_{46}^x &= \beta[-\Delta_6^x + 2\mu F_4^x(6) + \mu_\perp \sin \gamma E_1]; \\ z_{16}^y &= \beta[-\Delta_6^y + 2\mu F_1^y(6) + \mu_\perp \sin \gamma E_2], \\ z_{26}^y &= \beta[-\Delta_6^y + 2\mu F_2^y(6) - \mu_\perp \cos \gamma E_2], \\ z_{36}^y &= \beta[-\Delta_6^y + 2\mu F_3^y(6) - \mu_\perp \sin \gamma E_2], \\ z_{46}^y &= \beta[-\Delta_6^y + 2\mu F_4^y(6) + \mu_\perp \cos \gamma E_2]; \end{aligned} \quad (2.5)$$

μ_3 and μ_\perp are the longitudinal and transverse effective dipole moments of primitive cells, created by displacements and polarization of heavy ions which are triggered by deuteron ordering.

We took into account the following relations which are obeyed in the presence of stress σ_6 and fields E_i

$$\begin{aligned} \mu_{13} &= \mu_{23} = \mu_{33} = \mu_{43} = \mu_3, \\ \mu_{11} &= \mu_1 \cos \gamma, \quad \mu_{21} = -\mu_\perp \sin \gamma, \quad \mu_{12} = \mu_\perp \sin \gamma, \quad -\mu_{22} = \mu_\perp \cos \gamma; \\ \mu_{31} &= -\mu_\perp \cos \gamma, \quad \mu_{41} = \mu_\perp \sin \gamma, \quad \mu_{32} = -\mu_\perp \sin \gamma, \quad \mu_{42} = \mu_\perp \cos \gamma. \end{aligned} \quad (2.6)$$

Using the condition

$$\langle \sigma_{qf} \rangle^i = \frac{\text{Sp}\{\sigma_{qf} e^{-\beta \hat{H}_{q4}^{iA}(6)}\}}{\text{Sp}\{e^{-\beta \hat{H}_{q4}^{iA}(6)}\}} = \frac{\text{Sp}\{\sigma_{qf} e^{-\beta \hat{H}_{qf}^i(6)}\}}{\text{Sp}\{e^{-\beta \hat{H}_{qf}^i(6)}\}}, \quad (2.7)$$

where the single-particle deuteron Hamiltonians are

$$\hat{H}_{qf}^i(6) = -\frac{z_6^i \sigma_{qf}}{\beta}, \quad z_{f6}^i = -\beta \Delta_6^i + z_{f6}^i, \quad (2.8)$$

we calculate the single-particle distribution functions of deuterons and exclude the parameters Δ_6^i

$$\eta^{(1)z}(6) = \frac{m^z(6)}{D_6^z}, \quad (2.9)$$

where

$$\begin{aligned} m^z(6) &= \sinh(2z_6^z + \beta \delta_{s6} \varepsilon_6) + 2b \sinh(z_6^z - \beta \delta_{16} \varepsilon_6), \\ D_6^z &= \cosh(2z_6^z + \beta \delta_{s6} \varepsilon_6) + 4b \cosh(z_6^z - \beta \delta_{16} \varepsilon_6) + d + aa_6 + a/a_6, \\ z_6^z &= \frac{1}{2} \ln \frac{1 + \eta^{(1)z}(6)}{1 - \eta^{(1)z}(6)} + \beta \nu_c(6) \eta^{(1)z}(6) - \beta \psi_6 \varepsilon_6 + \frac{\beta \mu_3 E_3}{2}, \\ a &= \exp(-\beta \varepsilon), \quad b = \exp(-\beta w), \quad d = \exp(-\beta w_1), \quad a_6 = \exp(-\beta \delta_6 \varepsilon_6), \end{aligned} \quad (2.10)$$

also

$$\eta_f^{(1)\alpha}(6) = \frac{m_f^\alpha(6)}{D_f^\alpha(6)}, \quad (\alpha = x, y), \quad (2.11)$$

where

$$\begin{aligned} m_3^\alpha(6) &= \sinh\left(\frac{A_1^\alpha(6)}{2} + \beta \delta_{s6} \varepsilon_6\right) + d \sinh\left(\frac{A_2^\alpha(6)}{2}\right) \pm \\ & \pm aa_6 \sinh\left(\frac{A_3^\alpha(6)}{2}\right) \pm \frac{a}{a_6} \sinh\left(\frac{A_4^\alpha(6)}{2}\right) + \\ & + b \left[\pm \sinh\left(\frac{A_5^\alpha(6)}{2} - \beta \delta_{16} \varepsilon_6\right) \mp \sinh\left(\frac{A_6^\alpha(6)}{2} - \beta \delta_{16} \varepsilon_6\right) + \right. \end{aligned}$$

$$\begin{aligned}
& + \sinh\left(\frac{A_7^\alpha(6)}{2} - \beta\delta_{16}\varepsilon_6\right) + \sinh\left(\frac{A_8^\alpha(6)}{2} - \beta\delta_{16}\varepsilon_6\right) \Big], \\
m_4^\alpha(6) &= \sinh\left(\frac{A_1^\alpha(6)}{2} + \beta\delta_{s6}\varepsilon_6\right) - d \sinh\frac{A_2^\alpha(6)}{2} \pm \\
& \pm aa_6 \sinh\frac{A_3^\alpha(6)}{2} \mp \frac{a}{a_6} \sinh\frac{A_4^\alpha(6)}{2} + \\
& + b \left[\sinh\left(\frac{A_5^\alpha(6)}{2} - \beta\delta_{16}\varepsilon_6\right) + \sinh\left(\frac{A_6^\alpha(6)}{2} - \beta\delta_{16}\varepsilon_6\right) \pm \right. \\
& \left. \pm \sinh\left(\frac{A_7^\alpha(6)}{2} - \beta\delta_{16}\varepsilon_6\right) \mp \sinh\left(\frac{A_8^\alpha(6)}{2} - \beta\delta_{16}\varepsilon_6\right) \right] \quad (2.12) \\
D^\alpha(6) &= \cosh\left(\frac{A_1^\alpha(6)}{2} + \beta\delta_{s6}\varepsilon_6\right) + d \sinh\frac{A_2^\alpha(6)}{2} + \\
& + aa_6 \cosh\frac{A_3^\alpha(6)}{2} + \frac{a}{a_6} \cosh\frac{A_4^\alpha(6)}{2} + \\
& + b \left[\cosh\left(\frac{A_5^\alpha(6)}{2} - \beta\delta_{16}\varepsilon_6\right) + \cosh\left(\frac{A_6^\alpha(6)}{2} - \beta\delta_{16}\varepsilon_6\right) + \right. \\
& \left. + \cosh\left(\frac{A_7^\alpha(6)}{2} - \beta\delta_{16}\varepsilon_6\right) + \cosh\left(\frac{A_8^\alpha(6)}{2} - \beta\delta_{16}\varepsilon_6\right) \right]
\end{aligned}$$

Here the following notations are used

$$\begin{aligned}
A_1^\alpha(6) &= z_1^\alpha(6) \pm z_2^\alpha(6) + z_3^\alpha(6) \pm z_4^\alpha(6); \\
A_3^\alpha(6) &= z_1^\alpha(6) \pm z_2^\alpha(6) - z_3^\alpha(6) \mp z_4^\alpha(6); \\
A_5^\alpha(6) &= \pm z_1^\alpha(6) + z_2^\alpha(6) \mp z_3^\alpha(6) + z_4^\alpha(6); \\
A_7^\alpha(6) &= z_1^\alpha(6) \pm z_2^\alpha(6) + z_3^\alpha(6) \mp z_4^\alpha(6);
\end{aligned}$$

and

$$\begin{aligned}
z_{16}^x &= \frac{1}{2} \ln \frac{1 + \eta_1^{(1)x}(6)}{1 - \eta_1^{(1)x}(6)} + \beta\nu_1\eta_1^{(1)x}(6) + \beta\nu_3\eta_3^{(1)x}(6) + \\
& + \beta\nu_2\eta_2^{(1)x}(6) + \beta\nu_4\eta_4^{(1)x}(6) - \beta\psi_6\varepsilon_6 + \frac{\beta\mu_\perp \cos \gamma E_1}{2}, \\
z_{36}^x &= \frac{1}{2} \ln \frac{1 + \eta_3^{(1)x}(6)}{1 - \eta_3^{(1)x}(6)} + \beta\nu_3\eta_1^{(1)x}(6) + \beta\nu_1\eta_3^{(1)x}(6) + \\
& + \beta\nu_2\eta_2^{(1)x}(6) + \beta\nu_4\eta_4^{(1)x}(6) - \beta\psi_6\varepsilon_6 - \frac{\beta\mu_\perp \cos \gamma E_1}{2}, \quad (2.13) \\
z_{26}^x &= \frac{1}{2} \ln \frac{1 + \eta_2^{(1)x}(6)}{1 - \eta_2^{(1)x}(6)} + \beta\nu_2\eta_1^{(1)x}(6) + \beta\nu_2\eta_3^{(1)x}(6) +
\end{aligned}$$

$$\begin{aligned}
& + \beta\nu_1\eta_2^{(1)x}(6) + \beta\nu_3\eta_4^{(1)x}(6) - \beta\psi_6\varepsilon_6 - \frac{\beta\mu_\perp \sin \gamma E_1}{2}, \\
z_{46}^x &= \frac{1}{2} \ln \frac{1 + \eta_4^{(1)x}(6)}{1 - \eta_4^{(1)x}(6)} + \beta\nu_2\eta_1^{(1)x}(6) + \beta\nu_2\eta_3^{(1)x}(6) + \\
& + \beta\nu_3\eta_2^{(1)x}(6) + \beta\nu_1\eta_4^{(1)x}(6) - \beta\psi_6\varepsilon_6 + \frac{\beta\mu_\perp \sin \gamma E_1}{2}; \\
z_{16}^y &= \frac{1}{2} \ln \frac{1 + \eta_1^{(1)y}(6)}{1 - \eta_1^{(1)y}(6)} + \beta\nu_1\eta_1^{(1)y}(6) + \beta\nu_3\eta_3^{(1)y}(6) + \\
& + \beta\nu_2\eta_2^{(1)y}(6) + \beta\nu_2\eta_4^{(1)y}(6) - \beta\psi_6\varepsilon_6 - \frac{\beta\mu_\perp \sin \gamma E_2}{2}, \\
z_{36}^y &= \frac{1}{2} \ln \frac{1 + \eta_3^{(1)y}(6)}{1 - \eta_3^{(1)y}(6)} + \beta\nu_3\eta_1^{(1)y}(6) + \beta\nu_1\eta_3^{(1)y}(6) + \\
& + \beta\nu_2\eta_2^{(1)y}(6) + \beta\nu_2\eta_4^{(1)y}(6) - \beta\psi_6\varepsilon_6 + \frac{\beta\mu_\perp \sin \gamma E_2}{2}, \quad (2.14) \\
z_{26}^y &= \frac{1}{2} \ln \frac{1 + \eta_2^{(1)y}(6)}{1 - \eta_2^{(1)y}(6)} + \beta\nu_2\eta_1^{(1)y}(6) + \beta\nu_2\eta_3^{(1)y}(6) + \\
& + \beta\nu_1\eta_2^{(1)y}(6) + \beta\nu_3\eta_4^{(1)y}(6) - \beta\psi_6\varepsilon_6 - \frac{\beta\mu_\perp \cos \gamma E_2}{2}, \\
z_{46}^y &= \frac{1}{2} \ln \frac{1 + \eta_4^{(1)y}(6)}{1 - \eta_4^{(1)y}(6)} + \beta\nu_2\eta_1^{(1)y}(6) + \beta\nu_2\eta_3^{(1)y}(6) + \\
& + \beta\nu_3\eta_2^{(1)y}(6) + \beta\nu_1\eta_4^{(1)y}(6) - \beta\psi_6\varepsilon_6 + \frac{\beta\mu_\perp \cos \gamma E_2}{2}.
\end{aligned}$$

3. Elastic, piezoelectric, and dielectric properties of the KD_2PO_4 type crystals under the mechanic stress σ_6

Influence of the stress σ_6 on the characteristics of the KD_2PO_4 type crystals will be considered using the thermodynamic potential per primitive cell, which within the four-particle cluster approximation reads

$$\begin{aligned}
g_{1E}(6) &= \frac{\bar{v}}{2} c_{66}^{E0} \varepsilon_6^2 - \bar{v} e_{36}^0 \varepsilon_6 E_3 - \frac{\bar{v}}{2} \chi_{33}^{\varepsilon 0} E_3^2 + 2T \ln 2 + \\
& + 2\nu_c [\eta^{(1)z}(6)]^2 - 2T \ln [1 - (\eta^{(1)z}(6))^2] - 2T \ln D_6^z - \bar{v} \sigma_6 \varepsilon_6. \quad (3.1)
\end{aligned}$$

Let us mention the equation for the extremum of the thermodynamic potential g_{1E} with respect to $\eta^{(1)}$ coincides with Equation (2.9).

From the thermodynamic equilibrium conditions

$$\frac{1}{\bar{v}} \left(\frac{\partial g_{1E}(6)}{\partial \varepsilon_6} \right)_{E_3, \sigma_6} = 0, \quad \frac{1}{\bar{v}} \left(\frac{\partial g_{1E}(6)}{\partial E_3} \right)_{\sigma_6} = -P_3$$

we obtain

$$\begin{aligned} \sigma_6 &= c_{66}^E \varepsilon_6 - e_{36}^0 E_3 + \frac{4\psi_6}{\bar{v}} \frac{m^z(6)}{D_6^z} + \frac{2\delta_{a6}}{\bar{v}D_6^z} M_{a6} - \frac{2\delta_{s6}}{\bar{v}D_6^z} M_{s6} + \frac{2\delta_{16}}{\bar{v}D_6^z} M_{16}, \\ P_3 &= e_{36}^0 \varepsilon_6 + \chi_{33}^{\varepsilon_0} E_3 + 2 \frac{\mu}{\bar{v}} \frac{m^z(6)}{D_6^z}, \end{aligned} \quad (3.2)$$

where

$$M_{a6} = aa_6 - \frac{a}{a_6}, \quad M_{s6} = \sinh(2z_6^z + \beta\delta_{s6}\varepsilon_6), \quad M_{16} = 4b \sinh(z_6^z - \beta\delta_{16}\varepsilon_6).$$

From (3.2) we find the electric field

$$E_3 = -h_{36}^0 \varepsilon_6 + k_{33}^{\varepsilon_0} \left(P_3 - 2 \frac{\mu}{\bar{v}} \frac{m^z(6)}{D_6^z} \right), \quad (3.3)$$

where $h_{36}^0 = e_{36}^0 / \chi_{33}^{\varepsilon_0}$, $k_{33}^{\varepsilon_0} = 1 / \chi_{33}^{\varepsilon_0}$. Substituting the expression (3.3) into (3.2), we get

$$\begin{aligned} \sigma_6 &= c_{66}^{P_0} \varepsilon_6 - h_{36}^0 \left(P_3 - 2 \frac{\mu}{\bar{v}} \frac{m^z(6)}{D_6^z} \right) + \frac{4\psi_6}{\bar{v}} \frac{m^z(6)}{D_6^z} + \\ &+ \frac{2\delta_{a6}}{\bar{v}D_6^z} M_{a6} - \frac{2\delta_{s6}}{\bar{v}D_6^z} M_{s6} + \frac{2\delta_{16}}{\bar{v}D_6^z} M_{16}, \end{aligned} \quad (3.4)$$

where $c_{66}^{P_0} = c_{66}^E + e_{36}^0 h_{36}^0$.

Expressions (3.3) and (3.4) can also be obtained from the conditions

$$\frac{1}{\bar{v}} \left(\frac{\partial f}{\partial \varepsilon_6} \right)_{P_3} = \sigma_6, \quad \frac{1}{\bar{v}} \left(\frac{\partial f}{\partial P_3} \right)_{\varepsilon_6} = E_3,$$

whereas the free energy f is

$$f(6) = g_{1E}(6) - \bar{v}P_3E_3. \quad (3.5)$$

Substituting the expressions (3.1) and (3.3) into (3.5), we obtain

$$\begin{aligned} f(6) &= \frac{\bar{v}}{2} c_{66}^{P_0} \varepsilon_6^2 - \bar{v} h_{36}^0 \varepsilon_6 P_3 + \frac{\bar{v}}{2} k_{33}^0 P_3^2 - \frac{\bar{v}}{2} k_{33}^0 \left(2 \frac{\mu}{\bar{v}} \eta^{(1)z}(6) \right)^2 + \\ &+ 2T \ln 2 + 2\nu_c [\eta^{(1)z}(6)]^2 - 2T \ln [1 - (\eta^{(1)z}(6))^2] - 2T \ln D_6^z. \end{aligned} \quad (3.6)$$

Let us study now the influence of the stress σ_6 on piezoelectric, dielectric and elastic properties of KD_2PO_4 .

From the expression for the mean value of quasispin $\langle \sigma_{qf} \rangle$ (2.9) it follows that

$$\left(\frac{\partial \eta^{(1)}(6)}{\partial \varepsilon_6} \right)_{E_3} = \frac{\beta\theta_6}{D_6 - 2\varphi_6^\eta \varkappa_6},$$

where

$$\begin{aligned} \varkappa_6 &= \cosh(2z_6 + \beta\delta_{s6}\varepsilon_6) + b \cosh(z_6 - \beta\delta_{16}\varepsilon_6) - \eta^{(1)}(6)m(6), \\ r_6 &= \delta_{s6} \cosh(2z_6 + \beta\delta_{s6}\varepsilon_6) - 2b\delta_{16} \cosh(z_6 - \beta\delta_{16}\varepsilon_6) + \\ &+ \eta^{(1)z}(6) [-\delta_{s6}M_{s6} + \delta_{a6}M_{a6} + \delta_{16}M_{16}], \\ \varphi_6^\eta &= \frac{1}{1 - (\eta^{(1)}(6))^2} + \beta\nu_c, \quad \theta_6 = -2\varkappa_6\psi_6 + r_6. \end{aligned}$$

Hence, the coefficient of piezoelectric stress e_{36} is

$$e_{36} = - \left(\frac{\partial \sigma_6}{\partial E_3} \right)_{\varepsilon_6} = \left(\frac{\partial P_3}{\partial \varepsilon_6} \right)_{E_3} = e_{36}^0 + \frac{2\mu_3}{\bar{v}} \frac{\beta\theta_6}{D_6 - 2\varphi_6^\eta \varkappa_6}. \quad (3.7)$$

In the paraelectric phase at $\sigma_6 = 0$, the coefficient of piezoelectric stress e_{36} equals

$$e_{36}^+ = e_{36}^0 + \frac{\mu_3}{\bar{v}} \frac{2\beta[-2(1+b)\psi_6 + \delta_{s6} - 2b\delta_{16}]}{-1 + 2b + 2a + d - 2\beta\nu_c(1+b)}. \quad (3.8)$$

Differentiating the expression for polarization (3.2) with respect to the field E_3 at constant strain ε_6 we obtain dielectric susceptibility of a clamped crystal

$$\chi_{33}^\varepsilon = \left(\frac{\partial P_3}{\partial E_3} \right)_{\varepsilon_6} = \chi_{33}^0 + \bar{v} \frac{\mu^2}{v^2} \frac{1}{T} \frac{2\varkappa_6}{D_6 - 2\varphi_6^\eta \varepsilon^t a_6}. \quad (3.9)$$

Using the relations

$$\begin{aligned} (D_6 - 2\varkappa_6\varphi_6^\eta) \left(\frac{\partial \eta^{(1)}(6)}{\partial \varepsilon_6} \right)_{P_3} &= \beta\theta_6 + \beta\mu_3\varkappa_6 \left(\frac{\partial E_3}{\partial \varepsilon_6} \right)_{P_3}, \\ (D_6 - 2\varkappa_6\varphi_6^\eta) \left(\frac{\partial \eta^{(1)}(6)}{\partial \sigma_6} \right)_{E_3} &= \beta\theta_6 \left(\frac{\partial \varepsilon_6}{\partial \sigma_6} \right)_{E_3}, \end{aligned}$$

where $s_{66}^E = \left(\frac{\partial P_3}{\partial \sigma_6} \right)$ is the crystal compliance at constant electric field, we obtain the constant of piezoelectric stress h_{36} :

$$h_{36} = - \left(\frac{\partial E_3}{\partial \varepsilon_6} \right)_{P_3} = - \left(\frac{\partial \sigma_6}{\partial P_3} \right)_{\varepsilon_6} = \frac{e_{36}}{\chi_{33}^\varepsilon} \quad (3.10)$$

and the coefficient of the piezoelectric strain

$$d_{36} = e_{36}s_{66}^E. \quad (3.11)$$

From (3.2) and (3.4) we get the expressions for the elastic constant c_{66}^E at constant field

$$\begin{aligned} c_{66}^E &= \left(\frac{\partial \sigma_6}{\partial \varepsilon_6} \right)_{E_3} = c_{66}^{E0} + \frac{8\beta\psi_6 - \varkappa_6\psi_6 + r_6}{\bar{v}} \frac{4\varphi_6^\eta r_6^2}{D_6 - 2\varkappa_6\varphi_6^\eta} - \\ &- \frac{2\beta}{\bar{v}D_6} \left[\delta_{s6}^2 \cosh(2z_6 + \beta\delta_{s6}\varepsilon_6) + \delta_{a6}^2 \left(ac_6 + \frac{a}{c_6} \right) + 4b\delta_{16}^2 \cosh(z_6 - \beta\delta_{16}\varepsilon_6) \right] + \\ &+ \frac{2\beta}{\bar{v}D_6} [-\delta_{s6}M_{s6} + \delta_{a6}M_{a6} + \delta_{16}M_{16}]^2; \end{aligned} \quad (3.12)$$

and for the elastic constant c_{66}^P at constant polarization

$$c_{66}^P = c_{66}^E + e_{36}h_{36}. \quad (3.13)$$

In the paraelectric phase at $\sigma_6 = 0$ when $\eta^{(1)}(6) = 0$, the renormalized elastic constant for an unstrained crystal is

$$\begin{aligned} c_{66}^{E+} &= c_{66}^{E0} - \frac{4\psi_6}{\bar{v}T} \frac{-2(1+b)\psi_6 + \delta_{s6}}{\bar{v}T[-1+2b+2a-2\beta\bar{v}_c(1+b)]} + \\ &+ \frac{4\psi_6\delta_{s6}}{\bar{v}D_6^+T} - \frac{2}{\bar{v}T(1+4b+2a)} (\delta_{s6}^2 + 2a\delta_{a6}^2 + \delta_{16}). \end{aligned} \quad (3.14)$$

Hence, the relations (3.2)–(3.4) take the form

$$\begin{aligned} \sigma_6 &= c_{66}^E\varepsilon_6 - e_{36}E_3, & \sigma_6 &= c_{66}^P\varepsilon_6 - h_{36}P_3, \\ P_3 &= e_{36}\varepsilon_6 + \chi_{33}^\varepsilon E_3, & E_3 &= -h_{36}\varepsilon_6 + k_{33}^\varepsilon P_3, \end{aligned} \quad (3.15)$$

where $k_{33}^\varepsilon = 1/\chi_{33}^\varepsilon$ is the inverse dielectric susceptibility. These relations can be also obtained within the phenomenological approach, but we preferred to have the microscopic expressions for c_{66}^E , e_{36} , χ_{33}^ε , h_{36} .

From the system of equations (3.15) at $E_3 = \text{const}$

$$\begin{aligned} c_{66}^P \left(\frac{\partial \varepsilon_6}{\partial \sigma_6} \right)_{E_3} - h_{36} \left(\frac{\partial P_3}{\partial \sigma_6} \right)_{E_3} &= 1, \\ -h_{36} \left(\frac{\partial \varepsilon_6}{\partial \sigma_6} \right)_{E_3} + k_{33}^\varepsilon \left(\frac{\partial P_3}{\partial \sigma_6} \right)_{E_3} &= 0 \end{aligned} \quad (3.16)$$

we find the expressions for the coefficient of piezoelectric strain

$$d_{36} = \left(\frac{\partial P_3}{\partial \sigma_6} \right)_{E_3} = \frac{h_{36}}{c_{66}^P k_{33}^\varepsilon - h_{36}^2} = \frac{e_{36}}{c_{66}^P - e_{36}h_{36}} \quad (3.17)$$

and compliances at constant field

$$s_{66}^E = \left(\frac{\partial \varepsilon_6}{\partial \sigma_6} \right)_{E_3} = \frac{k_{33}^\varepsilon}{c_{66}^P k_{33}^\varepsilon - h_{36}^2} = \frac{1}{c_{66}^P - e_{36}h_{36}} = \frac{1}{c_{66}^E}. \quad (3.18)$$

From (3.15) at $P_3 = \text{const}$ we get

$$\begin{aligned} c_{66}^E \left(\frac{\partial \varepsilon_6}{\partial \sigma_6} \right)_{P_3} - e_{36} \left(\frac{\partial E_3}{\partial \sigma_6} \right)_{P_3} &= 1, \\ e_{36} \left(\frac{\partial \varepsilon_6}{\partial \sigma_6} \right)_{P_3} + \chi_{33}^\varepsilon \left(\frac{\partial E_3}{\partial \sigma_6} \right)_{P_3} &= 0; \end{aligned}$$

hence the constant of piezoelectric strain is

$$g_{36} = - \left(\frac{\partial E_3}{\partial \sigma_6} \right)_{P_3} = \frac{e_{36}}{\left(c_{66}^E + \frac{e_{36}^2}{\chi_{33}^\varepsilon} \right) \chi_{33}^\varepsilon} = \frac{h_{36}}{c_{66}^E + e_{36}h_{36}} = \frac{h_{36}}{c_{66}^P}, \quad (3.19)$$

and compliance at constant polarization is

$$s_{66}^P = \left(\frac{\partial \varepsilon_6}{\partial \sigma_6} \right)_{P_3} = \frac{1}{c_{66}^E + \frac{e_{36}^2}{\chi_{33}^\varepsilon}} = \frac{1}{c_{66}^P}. \quad (3.20)$$

Differentiating the system (3.15) with respect to the field E_3 at constant stress, we get

$$c_{66}^E \left(\frac{\partial \varepsilon_6}{\partial E_3} \right)_{\sigma_6} - e_{36} = 0, \quad -e_{36} \left(\frac{\partial \varepsilon_6}{\partial E_3} \right)_{\sigma_6} + \left(\frac{\partial P_3}{\partial E_3} \right)_{\sigma_6} = \chi_{33}^\varepsilon. \quad (3.21)$$

Since

$$d_{36} = \left(\frac{\partial \varepsilon_6}{\partial E_3} \right)_{\sigma_6},$$

then the dielectric susceptibility at $\sigma_6 = \text{const}$ is

$$\chi_{33}^\sigma = \left(\frac{\partial P_3}{\partial E_3} \right)_{\sigma_6} = \chi_{33}^\varepsilon + e_{36}d_{36}. \quad (3.22)$$

Hence, we obtained the microscopic expressions for c_{66}^E , e_{36} , and χ_{33}^ε ; the other characteristics are expressed via them.

Let us calculate now the transverse dielectric susceptibility of the KD_2PO_4 type crystals in the presence of stress σ_6 defined as

$$\begin{aligned} \chi_{11}^\varepsilon &= \frac{\mu_\perp \cos \gamma}{v} \left(\frac{\partial \eta_1^{(1)x}(6)}{\partial E_1} - \frac{\partial \eta_3^{(1)x}(6)}{\partial E_1} \right) + \\ &+ \frac{\mu_\perp \sin \gamma}{v} \left(-\frac{\partial \eta_2^{(1)x}(6)}{\partial E_1} + \frac{\partial \eta_4^{(1)x}(6)}{\partial E_1} \right). \end{aligned} \quad (3.23)$$

Using the relations (2.11)–(2.14) we obtain the following system of equations

$$\begin{aligned} & \beta\mu_{\perp}(\cos\gamma\kappa_6^a - M_{a6}\sin\gamma) = \\ & = (D_6 - \kappa_6^a\varphi_6^a)\frac{\partial(\eta_1^{(1)x}(6) - \eta_3^{(1)x}(6))}{\partial E_1} - M_{a6}\varphi_6^a\frac{\partial(\eta_4^{(1)x}(6) - \eta_2^{(1)x}(6))}{\partial E_1} \\ & \beta\mu_{\perp}(M_{a6}\cos\gamma - \sin\gamma\kappa_6^a) = \\ & = (D_6 - \kappa_6^a\varphi_6^a)\frac{\partial(\eta_4^{(1)x}(6) - \eta_2^{(1)x}(6))}{\partial E_1} - M_{a6}\varphi_6^a\frac{\partial(\eta_1^{(1)x}(6) - \eta_3^{(1)x}(6))}{\partial E_1}, \end{aligned}$$

where the following notations are used

$$\kappa_6^a = aa_6 + \frac{a}{a_6} + 2b\cosh(z_6 - \beta\delta_{16}\varepsilon_6), \quad \varphi_6^a = \frac{1}{1 - (\eta^{(1)}(6))^2} + \beta(\nu_1 - \nu_3).$$

In the result

$$\begin{aligned} \chi_{11}^{\varepsilon} &= \bar{v}\frac{\mu_{\perp}^2}{v^2}\frac{1}{T}\frac{(D_6 - \varphi_6^a\kappa_6^a)\kappa_6^a - \varphi_6^a M_{a6}^2}{(D_6 - \varphi_6^a\kappa_6^a)^2 - (\varphi_6^a M_{a6})^2} + \\ &- \bar{v}\frac{\mu_{\perp}^2}{v^2}\frac{1}{T}\frac{D\kappa_6}{(D_6 - \varphi_6^a\kappa_6^a)^2 - (\varphi_6^a M_{a6})^2}\sin 2\gamma. \end{aligned} \quad (3.24)$$

4. Influence of stress σ_6 on thermal properties of the KD_2PO_4 type crystals

Molar entropy of the deuteron subsystem of KD_2PO_4 type crystals under stress σ_6 reads

$$\begin{aligned} S_6 = -R\left(\frac{\partial f_6}{\partial T}\right)_{P_3, \varepsilon_6} &= R\left\{2\ln 2 + 2\ln[1 - (\eta^{(1)}(6))^2] + 2\ln D_6 + \right. \\ &+ \left. 4T\varphi_6^T\eta^{(1)}(6) + \frac{2M_6}{D_6}\right\}, \end{aligned} \quad (4.1)$$

where R is the gas constant, and

$$\begin{aligned} \varphi_6^T &= -\frac{1}{T^2}(\bar{v}_c\eta^{(1)}(6) - \psi_6\varepsilon_6), \\ M_6 &= 4b\frac{w}{T}\cosh z_6 + d\frac{w_1}{T} + \left(ac_6 + \frac{a}{c_6}\right)\frac{\varepsilon}{T} + \left(ac_6 - \frac{a}{c_6}\right)\frac{\delta_6\varepsilon_6}{T}. \end{aligned} \quad (4.2)$$

The molar specific heat of the deuteron subsystem of KD_2PO_4 type crystals can be calculated by differentiating the entropy

$$\Delta C_6^{\sigma} = T\left(\frac{\partial S}{\partial T}\right)_{\sigma} = \Delta C_6^{\varepsilon} + q_6^P\alpha_6, \quad (4.3)$$

where ΔC_6^{ε} is the molar specific heat at constant strain

$$\Delta C_6^{\varepsilon} = q_6^{P, \varepsilon} + q_6^{\varepsilon}p_6^{\sigma}. \quad (4.4)$$

Using the relations (4.1) we obtain

$$\begin{aligned} q_6^{P, \varepsilon} &= \left(\frac{\partial S_6}{\partial T}\right)_{P_3, \varepsilon_6} = \\ &= \frac{2R}{D_6}\left\{2T\varphi_6^T[2\kappa_6T\varphi_6^T + 2(q_6 - \eta^{(1)}(6)M_6)] + N_6 - \frac{M_6^2}{D_6}\right\}, \\ q_6^{\varepsilon} &= \left(\frac{\partial S_6}{\partial P_3}\right)_{\varepsilon_6, T} = \frac{v}{\mu_3}\frac{2RT}{D_6}\varphi_6^{\eta}\{2\kappa_6T\varphi_6^T + [q_6 - \eta^{(1)}(6)M_6]\} \end{aligned} \quad (4.5)$$

is the polarization heat at given ε_6 ,

$$\begin{aligned} q_6^P &= \left(\frac{\partial S_6}{\partial \varepsilon_6}\right)_{P_3, T} = \frac{2R}{D_6}\left\{2T\varphi_6^T(-2\kappa_6\psi_6 + r_6) - 2[q_6 - \eta^{(1)}(6)M_6]\psi_6 \right. \\ &- \left. \lambda_6 + \frac{M_6}{D_6}(-\delta_{s6}M_{s6} + \delta_{a6}M_{a6} + \delta_{16}M_{16})\right\}, \end{aligned}$$

is the deformation heat at given P_3 , where

$$\begin{aligned} N_6 &= \frac{1}{T^2}\left[(\varepsilon + \delta_{a6}\varepsilon_6)^2aa_6 + (\varepsilon - \delta_{a6}\varepsilon_6)^2\frac{a}{a_6} + 4bw^2\cosh(z_6^z - \beta\delta_{16}\varepsilon_6) + \right. \\ &+ w_1^2d - (\delta_{s6}\varepsilon_6)^2\cosh(2z_6 + \beta\delta_{as}\varepsilon_6) + \\ &+ \left. (\delta_{16}\varepsilon_6)^24b\cosh(z_6 - \beta\delta_{16}\varepsilon_6) + (\delta_{16}\varepsilon_6w)8b\cosh(z_6 - \beta\delta_{16}\varepsilon_6)\right], \\ q_6 &= \frac{1}{T}\left[-\delta_{s6}\varepsilon_6\cosh(2z_6 + \beta\delta_{as}\varepsilon_6) + \delta_{16}\varepsilon_62b\cosh(z_6 - \beta\delta_{16}\varepsilon_6) + \right. \\ &+ \left. 2bw\cosh(z_6 - \beta\delta_{16}\varepsilon_6)\right], \\ \lambda_6 &= \frac{1}{T}\left[-\delta_{s6}^2\varepsilon_6\sinh(2z_6 + \beta\delta_{as}\varepsilon_6) + \delta_{16}^2\varepsilon_64b\cosh(z_6 - \beta\delta_{16}\varepsilon_6) + \right. \\ &+ \left. \delta_{a6}\left(aa_6(\varepsilon + \delta_{a6}\varepsilon_6) - \frac{a}{a_6}(\varepsilon - \delta_{a6}\varepsilon_6)\right) + \delta_{16}w\varepsilon_64b\sinh(z_6 - \beta\delta_{16}\varepsilon_6)\right]. \end{aligned}$$

In (4.3) and (4.4) $p_6^{\sigma} = (\partial P_3/\partial T)_{\sigma, E_3}$ is the pyroelectric coefficient, and $\alpha_6 = (\partial \varepsilon_6/\partial T)_{\sigma}$ is the thermal expansion coefficient.

From relations (3.15) we get

$$p_6^\sigma = p_6^\varepsilon + e_{36}\alpha_6, \quad (4.6)$$

where

$$p_6^\varepsilon = \frac{\mu_3}{v} \frac{2 \kappa_6 T \varphi_6^T + [q_6 - \eta^{(1)}(6)M_6]}{D_6 - 2\kappa_6 \varphi_6^\eta}, \quad (4.7)$$

and the thermal expansion coefficient reads

$$\alpha_6 = \frac{-p_6 + h_{36}p_6^\varepsilon}{c_{66}^E}, \quad (4.8)$$

where $p_6 = \left(\frac{\partial \sigma_6}{\partial T}\right)_{p_3, \varepsilon_6} = q_6^p$ is the thermal pressure.

5. Discussion

Before going into the discussion of the proposed in previous sections theory, let us note that, strictly speaking, this theory can be valid for a completely deuterated KD_2PO_4 crystal only, whereas the vast majority of experimental data concerns the crystals, deuterated partially (see [15–20]). Nevertheless, as the relaxational character of dielectric dispersion in $\text{K}(\text{H}_{1-x}\text{D}_x)_2\text{PO}_4$ crystals implies, tunneling effects in them are most likely suppressed by the short-range correlations between hydrogens [21–23]. So at least in the case of high deuteration, we are allowed to neglect tunneling and apply the theory to partially deuterated crystals as well. Hereafter we shall consider the crystal with nominal deuteration $x = 0.89$ with the transition temperature $T_{C0} = 210.7$ K, for which experimental data for the relevant elastic, piezoelectric, and dielectric characteristics are available.

As the values of the theory parameters ε and w we choose those found in [24,25], which at $\sigma_6 = 0$ provide a satisfactory agreement of the calculated curves with the experimental data for spontaneous polarization, specific heat, static and dynamic dielectric permittivities of the crystal.

To determine the deformation potentials and “seed” quantities, we use the experimental data of [19,20] for the temperature dependences of the coefficient of piezoelectric strain d_{36} , dielectric susceptibility χ_{33} , and compliance s_{66}^E at $\sigma_6 = 0$. Using the known relations between dielectric, elastic and piezoelectric characteristics and having the values of d_{36} , χ_{33}^σ , and s_{66}^E we can calculate the piezoelectric constants e_{36} , h_{36} , g_{36} , elastic characteristics c_{66}^P , c_{66}^E , s_{66}^P , and dielectric susceptibility χ_{33}^ε .

Analogous calculations were carried out also for $x = 0$ using the data of [16–18]. Let us mention that the experimental values of d_{36} or c_{66}^E do not agree with the results presented in [15].

The deformation potentials ψ_6 and δ_{s6} , and the parameter of the long-range interaction ν were found from the condition that the transition temperature at $\sigma_6 = 0$ was $T_{C0} = 210.7$ K, and that the best description of the e_{36} , s_{66}^E , and ε_{33}^σ temperature curves was obtained. Let us note that we get the best fit if the following constraint

$$\delta_{s6} = 325 + 2\psi_6 \exp\left(-\frac{w}{T_{C0}}\right) \quad (5.9)$$

is held. By changing ψ_6 (or δ_{s6}) we can slightly alter the theoretical slopes $\partial h_{36}/\partial T$ and $\partial g_{36}/\partial T$ at $T > T_{C0}$. So, fitting the theoretical temperature dependences of the piezomodules h_{36} and g_{36} to experimental points, we choose the values of ψ_6 and δ_{s6} . It should, however, be noted that we can vary δ_{s6} rather strongly (from 0 up to the adopted in this paper value), provided Eq. 5.9 is obeyed, and still obtain a fair description of h_{36} and g_{36} .

The adopted value of the long-range interaction parameter is much lower than the one used in the theories where spontaneous strain is not taken into account [14]. Low ν allows us to describe the paraelectric Curie constant and ferroelectric spontaneous polarization with the same value of the effective dipole moment μ_3 strictly determined by the experimental saturation polarization.

The values of δ_{a6} and c_{66}^{E0} were chosen by fitting to experimental data the calculated $s_{66}^E(T)$ and $c_{66}^P(T)$ dependences. Moderate values of δ_{16} (splitting of the single-ionized deuteron configurations) do not perceptibly affect the calculated curves, and its larger values only make the fitting worse. Hence, for the sake of simplicity we neglect this splitting, taking $\delta_{16} = 0$.

The “seed” e_{36}^0 and $\chi_{33}^{\varepsilon 0}$ are merely the high temperature limits of experimental temperature dependences e_{36} and χ_{33}^ε .

The adopted values of the theory parameters are presented in Table 1.

Table 1. The theory parameters.

ε	w	ν_c	ψ_6	δ_{s6}	δ_{a6}	δ_{16}	$c_{66}^{E0} \cdot 10^{-10}$	μ_3/v	e_{36}^0	$\chi_{33}^{(0)}$
	(K)			(K)			(dyn/cm ²)	($\mu\text{C}/\text{cm}^2$)	(esu/cm ²)	
88.3	778	35.976	-250	1750	-187.5	0	7.0	6.21	$0.42 \cdot 10^4$	0.4

To find the order parameter $\eta^{(1)}$ and strain ε_6 we minimize the thermodynamic potential $g_{1E}(6)$ with respect to $\eta^{(1)}$ and determine ε_6 from Eq. (3.2).

Let us demonstrate how the presented theory describes the physical characteristics of the crystal related to the strain ε_6 and polarization P_3 at $\sigma_6 = 0$. As one can see, the theoretical results are in a good quantitative agreement with the experimental data in the paraelectric phase.

In fig. 2 we plot the dependence of the compliance s_{66}^E and elastic constants c_{66}^E and c_{66}^P of the $\text{K}(\text{H}_{0.11}\text{D}_{0.89})_2\text{PO}_4$ crystal on $\Delta T = T - T_C$ at $\sigma_6 = 0$. Here we also presented the experimental data for $x = 0.89$ [20] and $x = 0.00$ [15,18]. As one can see, the theoretical results are in a good quantitative agreement with the experimental data of [20] in the paraelectric phase. The compliance s_{66}^E at $T \rightarrow T_C$ has an anomalous increase, whereas the elastic constant c_{66}^E vanishes at the Curie point. The elastic constant c_{66}^P at $T < T_C$ is nearly constant with temperature, only has an about 6% decrease at $T = T_C$, and slightly increases in the paraelectric phase. That accords with the conclusions of [30], where it was shown that the ferroelectric phase transition in KH_2PO_4 did not affect the magnitude of s_{66}^E , and hence of c_{66}^E . According to the data of [15], at $x = 0.0$ the elastic constant c_{66}^P slightly decreases with temperature in the paraelectric phase.

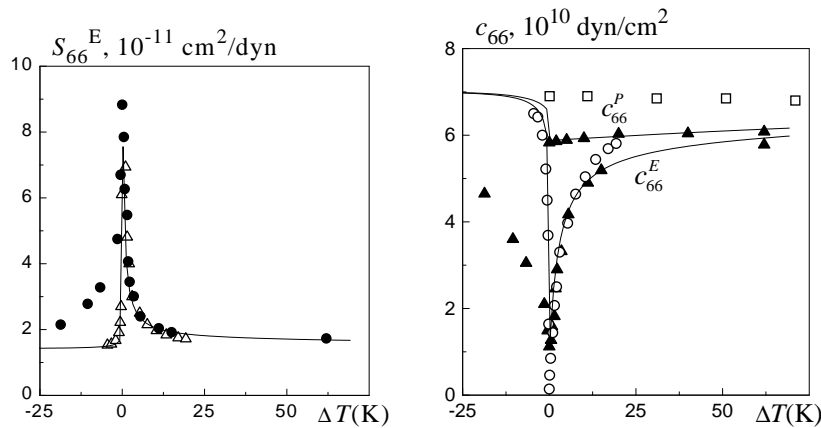


Figure 2. Temperature dependence of compliance s_{66}^E : \bullet - [20], Δ - $s_{66}^E = 1/c_{66}^E$ [18] and elastic constants c_{66}^P and c_{66}^E : \blacktriangle - $c_{66}^E = 1/s_{66}^E$ [20], $c_{66}^P = \frac{1}{s_{66}^E} + d_{36}^2/S_{66}^E \chi_{33}^\varepsilon$ [19,20]; \circ - [18]; \square - [15].

Temperature dependence of the coefficient of piezoelectric strain d_{36}

and coefficient of piezoelectric stress e_{36} of the $\text{K}(\text{H}_{0.11}\text{D}_{0.89})_2\text{PO}_4$ crystal at $\sigma_6 = 0$ is shown in fig. 3. A satisfactory agreement of the presented theory with the experimental data of [19] for d_{36} and with the data obtained from the formula $e_{36} = d_{36}[19]/s_{66}^E[20]$ is observed. At $T \rightarrow T_C$ coefficients d_{36} and e_{36} sharply increase. In the ferroelectric phase, the calculated coefficients d_{36} and e_{36} sharply decrease with a rate much higher than in the paraelectric phase.

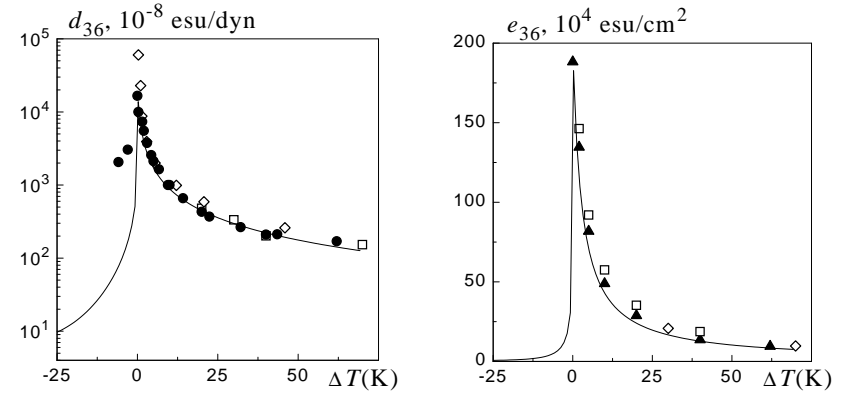


Figure 3. Temperature dependence of coefficient of piezoelectric strain d_{36} (left, experimental points taken from [19] - \bullet ($x = 0.89$), [16,17] - \diamond ($x = 0.00$), [15] - \square ($x = 0.00$)) and coefficient of piezoelectric stress $e_{36} = \frac{d_{36}[19]}{s_{66}^E[20]}$; \diamond - [16,17], \square - [15]).

Temperature dependence of the calculated constant of piezoelectric stress h_{36} and constant of piezoelectric strain g_{36} at $\sigma_6 = 0$ is shown in fig. 4 along with the obtained using the experimental data of [18, 19] values of h_{36} and g_{36} for $x = 0.89$ and the data of [15] for $x = 0.00$. The piezoelectric constants h_{36} or g_{36} do not have singularities at the ferroelectric transition; therefore they are called “true” piezoelectric constants of the crystals.

In fig. 5 we plot the temperature dependences of the dielectric permittivities of a free (ε_{33}^σ) and clamped ($\varepsilon_{33}^\varepsilon$) crystals at $\sigma_6 = 0$ along with the experimental data of [19] for ε_{33}^σ . The “experimental” data for the dielectric permittivity $\varepsilon_{33}^\varepsilon$ were calculated using the relation $\varepsilon_{33}^\varepsilon = \varepsilon_{33}^\sigma - 4\pi e_{36}d_{36}$.

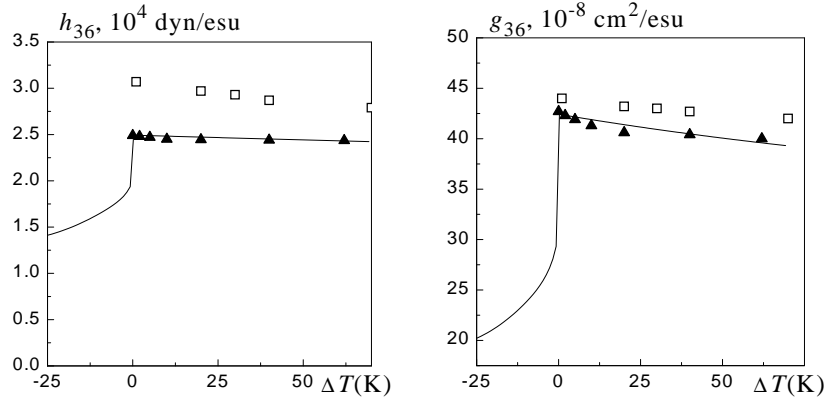


Figure 4. Temperature dependence of constant of piezoelectric stress h_{36} (left, \blacktriangle – $h_{36} = d_{36}[19]/S_{66}^E\chi_{33}^E[20]$, \square – [15]) and constant of piezoelectric strain g_{36} (right, \blacktriangle – $g_{36} = d_{36}/\chi_{33}^E$ [5], \square – [15]).

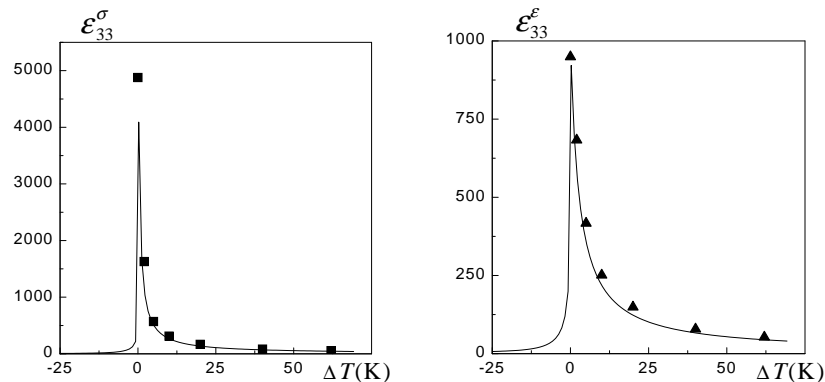


Figure 5. Temperature dependence of dielectric permittivity of a free crystal ϵ_{33}^σ (left, \blacksquare – [19]) and dielectric permittivity of a clamped crystal ϵ_{33}^ϵ (right, \blacktriangle – $\epsilon_{33}^\epsilon = \epsilon_{33}^\sigma - \frac{d_{36}^2}{S_{66}^E}$ [19,20]).

The presented graphs indicate that one can describe the temperature peculiarities of these dielectric, piezoelectric, and elastic properties of KD_2PO_4 attributing those peculiarities to deuteron subsystem only,

with the heavy ions lattice counterpart considered as background and temperature independent one. However, since we cannot unambiguously set the values of ψ_6 and δ_{s6} , we are not in position to determine what are the relative weights in these peculiarities of piezoelectric coupling, described by the parameter ψ_6 , and of the short-range up-down deuteron configurations splitting, induced by strain σ_6 and described by the parameter δ_{s6} .

In fig. 6 the dependences of the thermodynamic potential g_{1E} on the order parameter $\eta^{(1)}$ at different values of temperature and stress σ_6 are presented. The behavior of g_{1E} at zero stress σ_6 is usual for the first order phase transition: a little below the transition point g_{1E} has three minima – one at $\eta^{(1)} = 0$ and two symmetric ones $\pm\eta^{(1)} \neq 0$. The last two are of the same depth and lower than the one at $\eta^{(1)} = 0$. At $T = T_C$ all minima are of the same depth (criterion of the phase transition), and at $T > T_C$ the central minimum becomes the deepest. At higher temperatures the minima of g_{1E} at $\eta^{(1)} \neq 0$ disappear.

Under stress σ_6 , the dependence of $g_{1E}(\eta^{(1)})$ becomes asymmetric; the lower values of the thermodynamic potential are at those values of the order parameter, the sign of which coincide with the sign of the stress.

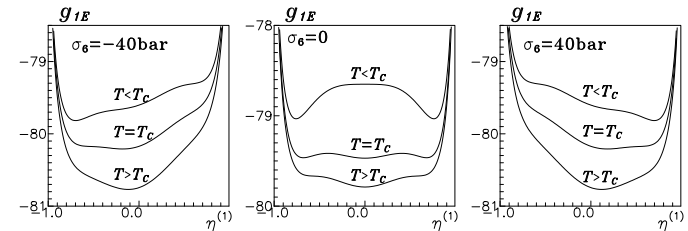


Figure 6. Dependences of the thermodynamic potential g_{1E} on the order parameter $\eta^{(1)}$ at different values of stress σ_6 .

In fig. 7 we plot the dependences of the solutions of the equation for the thermodynamic potential g_{1E} extremum and the corresponding values of g_{1E} on temperature at different values of stress σ_6 in the vicinity of the transition point.

Equation (2.9) may have up to five different solutions, three of which correspond to minima, and two correspond to maxima of the thermodynamic potential. One of the minima – the central one – is at small values of the order parameter, and the sign of $\eta^{(1)}$ coincides with

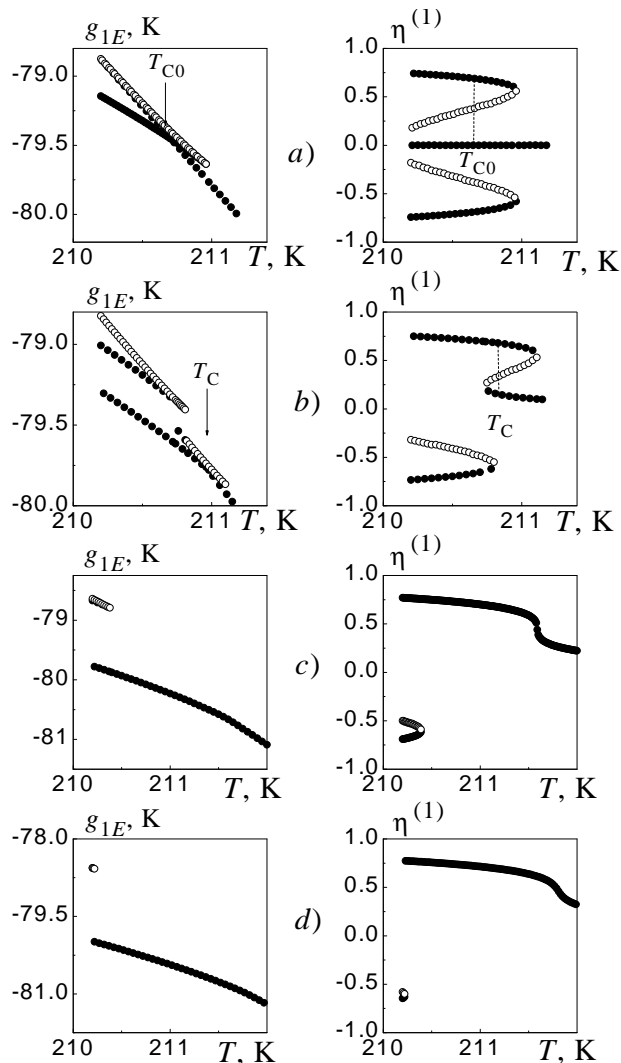


Figure 7. Temperature dependences of the thermodynamic potential and solutions of equation for the order parameter at different values of stress σ_6 : a) 0 bar, b) 40 bar, c) 77 bar, d) 100 bar. \circ and \bullet correspond to maxima and minima of the thermodynamic potential, respectively.

the sign of the stress σ_6 . The two other minima, if they exist, are nearly symmetric (absolutely symmetric at $\sigma_6 = 0$), and, as we have already mentioned, that minimum, the sign of which coincides with the sign of the stress is deeper.

Let $\eta_1^{(1)} < 0$, $\eta_2^{(1)} \approx 0$, and $\eta_3^{(1)} > 0$ be the possible solutions of Equation (2.9), corresponding to the minima of g_{1E} . As one can see (fig. 7), at $\sigma_6 > 0$

$$g_{1E}(\eta_3^{(1)}) < g_{1E}(\eta_2^{(1)}) \text{ at } T < T_C,$$

$$g_{1E}(\eta_3^{(1)}) = g_{1E}(\eta_2^{(1)}) \text{ at } T = T_C, \text{ (the phase transition criterion)}$$

$$g_{1E}(\eta_3^{(1)}) > g_{1E}(\eta_2^{(1)}) \text{ at } T > T_C.$$

The temperature of the first order phase transition at which the branches of the thermodynamic potential intersect, increases with stress σ_6 , and the values of $\eta_2^{(1)}$ at the transition point increase, whereas $\eta_3^{(1)}$ decrease. A decrease in the magnitude of jump in the order parameter $\delta\eta^{(1)} = \eta_3^{(1)} - \eta_2^{(1)}$ means that the order of the phase transition is moving towards to the second order. At certain stress σ_6^* $\delta\eta^{(1)}$ turns to zero – there is a critical point where the second order phase transition takes place (at T^*). Further increase in stress smears off the phase transition and results in continuous and smooth temperature dependence of the order parameter. Such behavior is typical for the first order phase transitions in ferroelectrics to which the electric field conjugate to spontaneous polarization is applied [26].

Corresponding $T_C - \sigma_6$ phase diagram is depicted in fig.8. Only the stable phases corresponding to absolute minima of thermodynamic potential are shown. The following temperatures are indicated: $T_{C0} = 210.7$ K is the temperature of the first order phase transition at $\sigma_6 = 0$; $T^* = 211.6$ K is the temperature of the second order phase transition at the critical point at stress $\sigma_6^* = 75$ bar; $T_0 = 210.8$ K is the Curie temperature of a free crystal $\sigma_6 = 0$, at which the compliance s_{66}^E and the longitudinal static dielectric permittivity ε_{33}^σ diverge. As one can see, the diagram is symmetric with respect to a change $\sigma_6 \rightarrow -\sigma_6$. An increase in the transition temperature with stress σ_6 is practically linear with the slope $\partial T_C / \partial |\sigma_6| = 21.6$ K/kbar, which is much faster with than with hydrostatic or uniaxial $p = -\sigma_3$ pressure [13].

The observed “Y”-shaped form of the phase diagram is not unique but typical for the systems in fields conjugate to the order parameter. The $T_C - E_3$ phase diagram of KH_2PO_4 of the same topology was obtained within the phenomenological approach without invoking any microscopic model by Schmidt [27]; an increase in the transition temper-

ature with E_3 and cease of the transition at certain critical E_3^* were observed experimentally in KD_2PO_4 by Sidnenko and Gladkii [29].

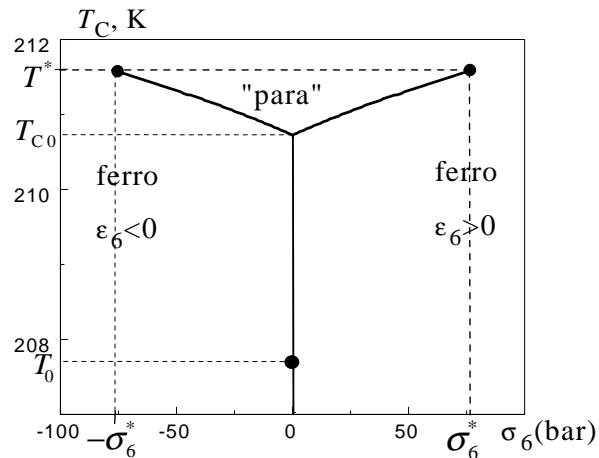


Figure 8. $T_C - \sigma_6$ phase diagrams of a KD_2PO_4 crystal.

Let us note that in order to observe the dependence of temperature phase transition on stress σ_6 experimentally, one should apply an external stress to the *paraelectric* crystal and cool it below the transition point. In absence of external fields or stresses, crystal at the transition can with 50:50 probability have positive or negative spontaneous strain. However, since in the presence of the stress σ_6 the minimum of the thermodynamic potential at $\eta^{(1)}$ of the same sign as that of σ_6 is deeper than the opposite minimum, the sign of the strain below the transition point will coincide with the sign of stress (similarly, as the direction of polarization in a crystal coincides with the direction of external field). The same picture will take place if the stress is applied to *spontaneously polarized and strained* crystal, provided that this stress induces the strain of the same sign as that of the spontaneous strain. However, if stress is applied to *spontaneously polarized and strained* crystal such that the signs of the stress induced and spontaneous strains are opposite, the system appears in a local minimum of the potential (for instance, at $\sigma_6 > 0$ $g_{1E}(\eta_1^{(1)}) > g_{1E}(\eta_3^{(1)})$), that is, in a metastable state. To predict theoretically when the transition to a stable state (which requires switching of polarization and strain) is impossible. Temperature of such a transition will essentially depend on the experimental conditions. Nevertheless, we

can maintain that this temperature is not higher than the temperature of absolute instability (the point where the local minimum disappears), and, as one can see at Figure 7, the temperature of absolute instability decreases with stress σ_6 .

Let us consider now the dependences of the values of the order parameter corresponding to minima of the thermodynamic potential on stress σ_6 at different values of temperature in the vicinity of the transition point, depicted in fig. 9. At $T < T_{C0}$, the branches of the thermodynamic potential $g_{1E}(\eta_1^{(1)} < 0)$ and $g_{1E}(\eta_3^{(1)} > 0)$ intersect, and the solutions of Equation (2.9) $\eta_1^{(1)}$ and $\eta_3^{(1)}$ can exist simultaneously. Experimentally, on changing stress σ_6 a regular hysteresis loop $P_3 - \sigma_6$ should be observed.

At $T_{C0} < T < T^*$, only one of the non-zero minima and the central minimum of the thermodynamic potential ($\eta_1^{(1)}$ and $\eta_2^{(1)}$ or $\eta_3^{(1)}$ and $\eta_2^{(1)}$) can coexist. Experiment should reveal a double hysteresis loop. At temperatures higher than the critical T^* , the dependences $g_{1E}(\sigma_6)$ and $\eta^{(1)}(\sigma_6)$ are smooth, and no jump in the order parameter is observed. Let us note that such a sequence of the hysteresis loops – a single loop at $T < T_{C0}$, a double loop at $T_{C0} < T < T^*$, and a gradual change at $T > T^*$ – was obtained yet by Merz for BaTiO_3 in electric field [28] and by Sidnenko and Gladkii [29] for KD_2PO_4 in the field E_3 , and is, apparently, typical for the phase order phase transitions in ferroelectrics under fields conjugate to the order parameter.

In fig. 10 we present the temperature and stress dependences of strain ε_6 at different values of stress σ_6 and different values of temperature. Fig. 11 illustrates the analogous dependences of polarization P_3 . As one can see, these quantities exhibit the identical variation with temperature or stress. The spontaneous strain ε_6 and polarization P_3 at $\sigma_6 = 0$ in the ferroelectric phase slightly decrease with temperature and jump to zero at $T = T_C$. When stress σ_6 is applied, the magnitudes of strains ε_6 and polarization P_3 increase, whereas the jumps $\Delta\varepsilon_6$ and ΔP_3 decrease; at $\sigma_6 = \sigma_6^*$ and $T = T_C^*$, the jumps vanish. At $\sigma_6 \neq 0$ ε_6 and P_3 differ from zero above the phase transition and slightly decrease with temperature. At $T_C < T < T_C^*$ values of ε_6 and P_3 increase with stress σ_6 , having upward jumps at stresses corresponding to the curve of phase equilibrium with $\Delta\varepsilon_6$ and ΔP_3 decreasing with stress and vanishing at $\sigma_6 = \sigma_6^*$.

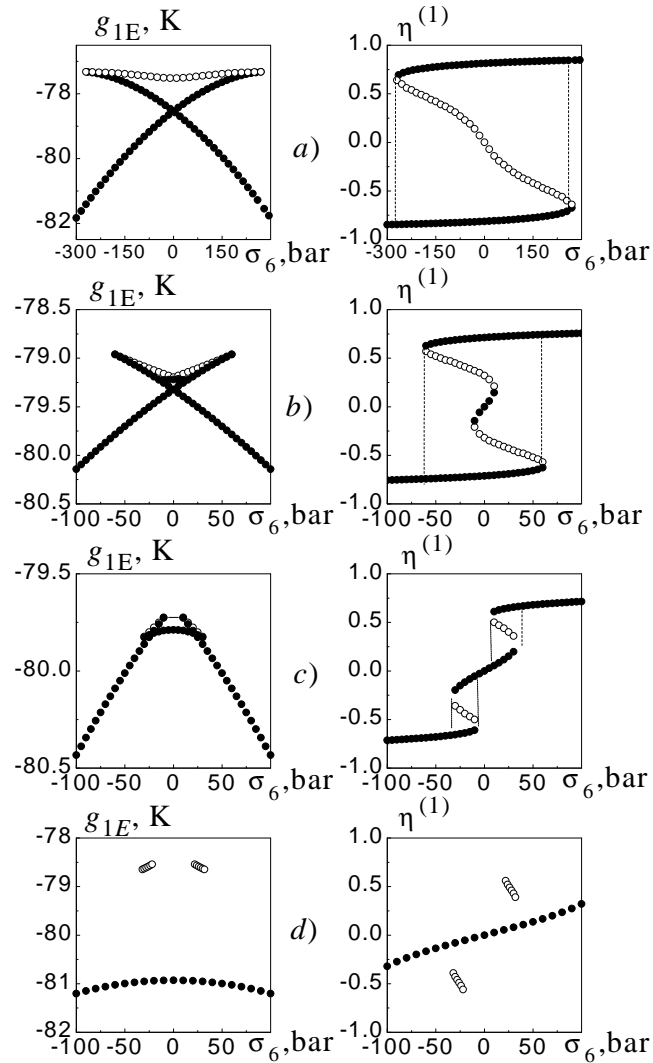


Figure 9. Stress dependences of the thermodynamic potential and solutions of equation for the order parameter at different values of temperature: a) 209 K, b) 210.5 K, c) 211 K, d) 212 K. $T_{C0} = 210.7$ K. \circ and \bullet correspond to maxima and minima of the thermodynamic potential, respectively.

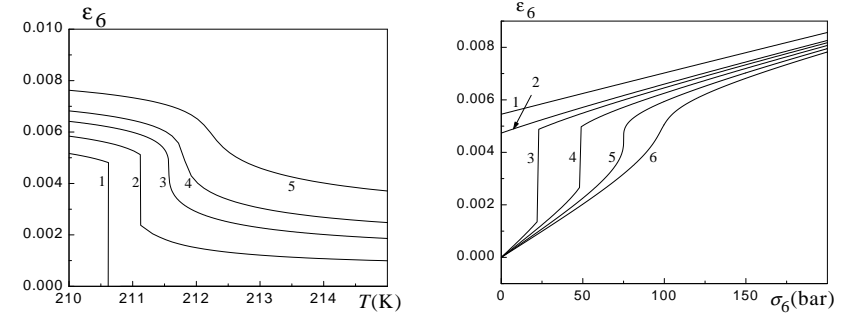


Figure 10. Dependences of strain ε_6 on temperature at different values of stress σ_6 (bar) (left): 1 - 0; 2 - 40; 3 - 40; 4 - 100; 5 - 150 and on stress σ_6 at different values of temperature T (K) (right): 1 - 209.0; 2 - $T_{C0} = 210.7$; 3 - 211; 4 - 211.3; 5 - $T^* = 211.57$; 6 - 211.8.

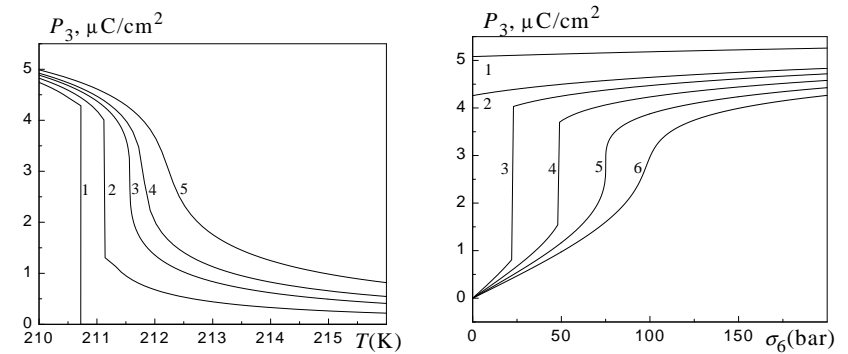


Figure 11. Dependences of polarization P_3 on temperature at different values of stress σ_6 (bar) (left): 1 - 0; 2 - 40; 3 - $\sigma_6^* = 75$; 4 - 100; 5 - 150 and on stress σ_6 at different values of temperature T (K) (right): 1 - 209.0; 2 - $T_{C0} = 210.7$; 3 - 211; 4 - 211.3; 5 - $T^* = 211.57$; 6 - 211.8.

Further increase in stress slightly raises up the strain ε_6 and polarization P_3 . At temperatures $T < T_C$ and $T - T_C > 3$ K values of ε_6 and P_3 exhibit a nearly linear increase with stress σ_6 . At changing the sign of the stress σ_6 , the absolute values of the strain ε_6 and polarization P_3 do not change, but become negative.

Let us discuss the theoretical results for the stress influence on the physical characteristics of the $\text{K}(\text{H}_{0.11}\text{D}_{0.89})_2\text{PO}_4$ crystal. The major stress σ_6 effects on the physical characteristics are related to the changes induced by this stress in the character of the phase transition and, therefore, essential only in the vicinity of the transition point; at $|T - T_C| > 5$ K, these effects are negligibly small.

In fig. 12 we plot the temperature and stress dependences of the elastic constant c_{66}^P at different values of stress σ_6 and temperature. As one can see, the elastic constant c_{66}^P change with temperature and stress exactly as the strain ε_6 and polarization P_3 do.

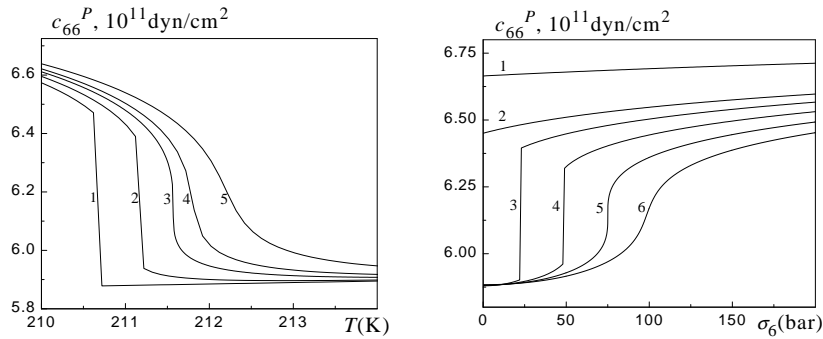


Figure 12. Dependences of elastic constant c_{66}^P on temperature at different values of stress σ_6 (bar) (left): 1 - 0; 2 - 40; 3 - $\sigma_6^* = 75$; 4 - 100; 5 - 150 and on stress σ_6 at different values of temperature T (K) (right): 1 - 209.0; 2 - $T_{C0} = 210.7$; 3 - 211; 4 - 211.3; 5 - $T^* = 211.57$; 6 - 211.8.

Temperature dependences of compliance s_{66}^E (fig. 13), coefficient of the piezoelectric strain d_{36} and stress e_{36} (fig. 14), and of the dielectric permittivity $\varepsilon_{33}^\varepsilon$ (fig. 15) at different values of stress σ_6 are similar. The maxima of these characteristics shift to higher temperatures with stress. At $\sigma_6 < \sigma_6^*$, these characteristics reaches their maximal values at the transition temperatures. At $\sigma_6 = \sigma_6^*$ i $T = T_C^*$ the second order phase transition takes place accompanied by a sharp increase in these quantities.

The temperature curves of the constants of piezoelectric stress g_{36} and piezoelectric strain g_{36} (fig. 16) at different values of stress σ_6 are similar to each other. At $\sigma_6 < \sigma_6^*$, minor jumps in h_{36} and g_{36} are observed, which vanish at $\sigma_6 = \sigma_6^*$. At $\sigma_6 > \sigma_6^*$ h_{36} i g_{36} increase with temperature, tending asymptotically to the values of h_{36} , g_{36} at $\sigma_6 = 0$.

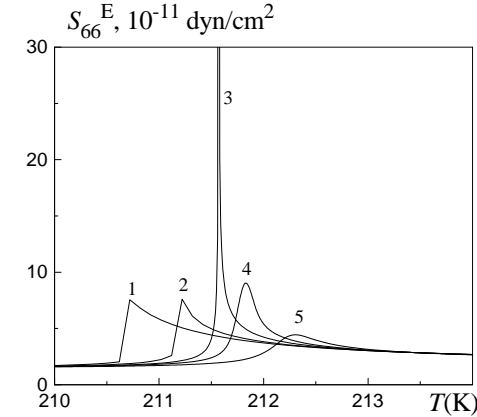


Figure 13. Temperature dependence of compliance s_{66}^E at different values of σ_6 (bar): 1 - 0; 2 - 40; 3 - $\sigma_6^* = 75$; 4 - 100; 5 - 150.

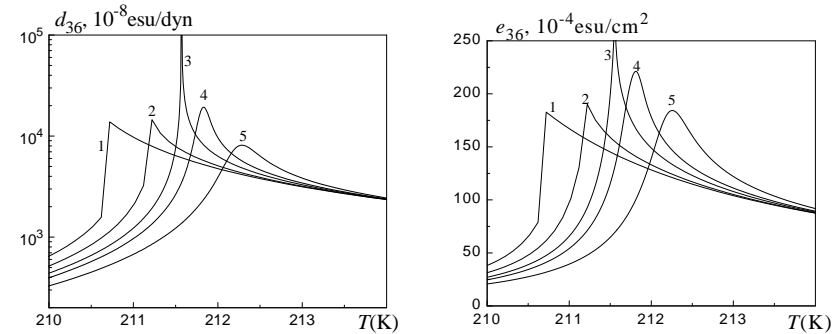


Figure 14. Temperature dependences of coefficient of piezoelectric strain d_{36} and coefficient of piezoelectric stress e_{36} at different values of stress σ_6 (bar): 1 - 0; 2 - 40; 3 - $\sigma_6^* = 75$; 4 - 100; 5 - 150.

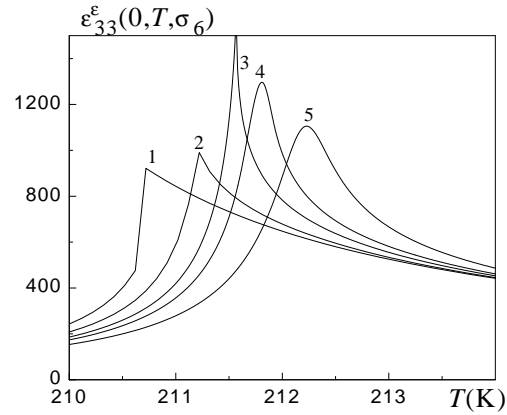


Figure 15. Dependences of dielectric permittivity ε_{33}^e on temperature at different values of stress σ_6 (bar): 1 - 0; 2 - 40; 3 - $\sigma_6^* = 75$; 4 - 100; 5 - 150.

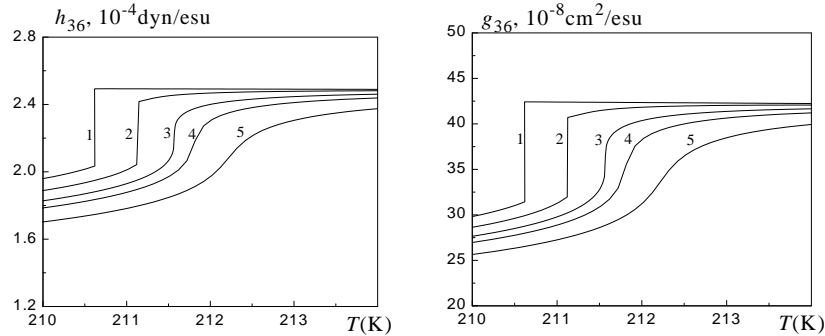


Figure 16. Temperature dependence of constant of piezoelectric stress h_{36} and constant of piezoelectric strain g_{36} at different values of stress σ_6 (bar): 1 - 0; 2 - 40; 3 - $\sigma_6^* = 75$; 4 - 100; 5 - 150.

The stress dependences of the compliance s_{66}^E , coefficients of piezoelectric strain d_{36} , piezoelectric stress e_{36} , dielectric permittivity ε_{33}^e at different values of temperature are presented in figs. 17, 18, 19.

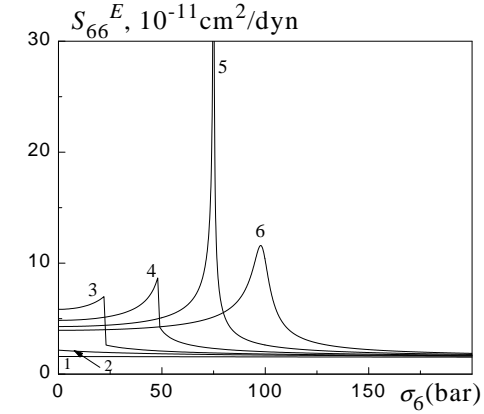


Figure 17. Dependences of compliance s_{66}^E on stress σ_6 at different values of temperature T (K): 1 - 209.0; 2 - $T_{C0} = 210.7$; 3 - 211; 4 - 211.3; 5 - $T^* = 211.57$; 6 - 211.8.

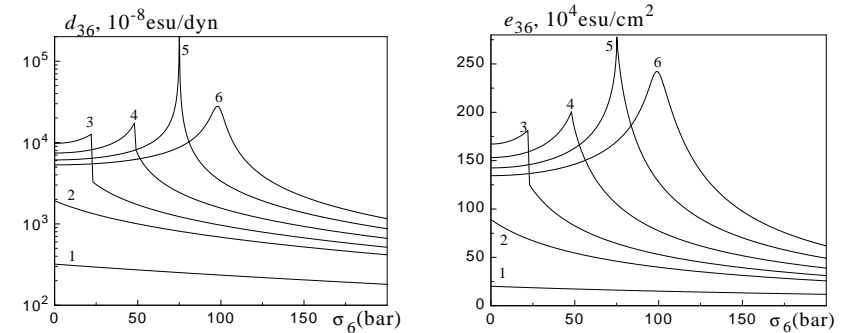


Figure 18. Dependences of coefficient of piezoelectric strain d_{36} and coefficient of piezoelectric stress e_{36} on stress σ_6 at different temperatures T (K): 1 - 209.0; 2 - $T_{C0} = 210.7$; 3 - 211; 4 - 211.3; 5 - $T^* = 211.57$; 6 - 211.8.

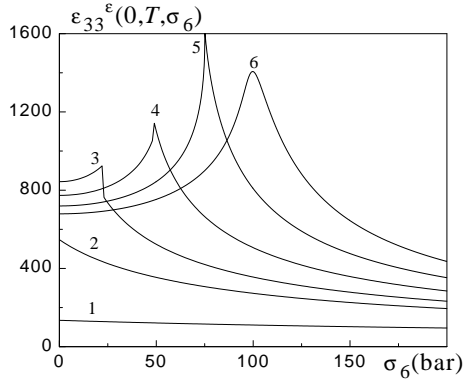


Figure 19. Dependences of dielectric permittivity ε_{33}^e on stress σ_6 at different values of temperature T (K): 1 - 210.0; 2 - $T_{C0} = 210.7$; 3 - 211; 4 - 211.3; 5 - $T^* = 211.57$; 6 - 211.8.

At temperatures below T_C , these characteristics decrease with stress σ_6 , decreasing being the stronger, the closer temperature is to T_{C0} . At $T_{C0} < T < T_C^*$, the mentioned characteristics increase with stress σ_6 , having downward jumps at stresses corresponding to the curve of phase equilibrium, with the jumps vanishing at $T = T_C^*$ and $\sigma_6 = \sigma_6^*$. The further increase in stress lowers down s_{66}^E , d_{36} , e_{36} and ε_{33}^e . At $T > T_C^*$, these quantities exhibit a gradual increase with stress, reach their maxima, and decrease on further increase in stress. As temperature rises, the maximal values of the quantities decrease and shift to higher stresses. At $\Delta T \geq 15$ K, the values of s_{66}^E , d_{36} , e_{36} , and ε_{33}^e are stress σ_6 independent.

In fig.20 we depict the dependences of constants of piezoelectric stress h_{36} and piezoelectric strain g_{36} on stress σ_6 at different values of temperature. At temperatures $T \leq T_C$ the values of h_{36} and g_{36} decrease with stress σ_6 . If $T_C < T < T_C^*$, the constants h_{36} and g_{36} are slightly lowered down by stress. At stresses corresponding to the curve of phase equilibrium they decrease with a jump, and at $\sigma_6 = \sigma_6^*$ the jump magnitude turns to zero, and the further increase in stress gives rise to an almost linear decrease in h_{36} and g_{36} . At temperatures $T > T_C^*$ h_{36} and g_{36} exhibit a gradual decrease with stress σ_6 .

Let us consider now the temperature and stress dependence of the transverse dielectric permittivity ε_{11} . Calculations were carried out at $\nu_1 - \nu_3 = 10$ K, $\mu_{\perp} = 2.79 \cdot 10^{-18}$ esu · cm, $\varepsilon_{\infty} = 10$. In fig.21 we depict the dependence of ε_{11} on temperature at different values of stress σ_6 and

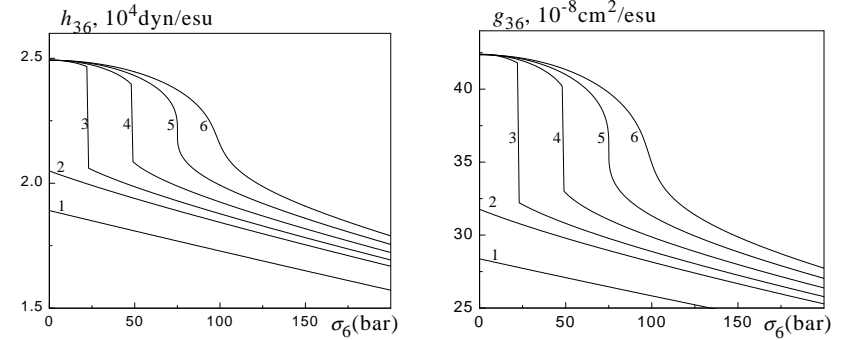


Figure 20. Dependences of constant of piezoelectric stress h_{36} and constant of piezoelectric strain g_{36} on stress σ_6 at different values of temperature T (K): 1 - 209.0; 2 - $T_{C0} = 210.7$; 3 - 211; 4 - 211.3; 5 - $T^* = 211.57$; 6 - 211.8.

on stress at different values of temperature along with the experimental points for $\sigma_6 = 0$.

In the paraelectric phase, the experimental data are described by the theory rather well. As temperature rises, ε_{11} gradually increases in the ferroelectric phase, has an upward jump at at the transition temperature, the jump magnitude being equal to zero at $\sigma_6 = \sigma_6^*$. At $\sigma_6 = 0$ the values of ε_{11} slightly decreases with temperature in the paraelectric phase, whereas at $\sigma_6 \neq 0$ after the upward jumps it asymptotically tends to the values of ε_{11} at $\sigma_6 = 0$. At $\sigma_6 = \sigma_6^*$ ε_{11} exhibits only smooth increase with temperature.

At temperatures $T < T_C$, the magnitude of ε_{11} is lowered down by stress σ_6 . If $T_C < T < T_C^*$, ε_{11} slightly decreases with stress, then at stresses corresponding to the curve of phase equilibrium it has a downward jump, the size of which $\Delta\varepsilon_{11}$ is zero at $\sigma_6 = \sigma_6^*$. At further increase in stress σ_6 , ε_{11} decreases linearly. At $T > T_C^*$ the permittivity ε_{11} exhibits a smooth decrease with stress σ_6 .

In fig.22 we plot the dependence of specific heat of a deuteron subsystem of $K(H_{0.11}D_{0.89})_2PO_4$ on temperature at different values of stress σ_6 and dependence of ΔC_6^σ on stress σ_6 at different values of temperature.

In the ferroelectric phase at $\sigma_6 = 0$, the magnitude of ΔC_6^σ increases as temperature approaches T_C , has a downward jump at the transition point, and is nearly constant in the paraelectric phase. On increasing stress σ_6 up to σ_6^* , the maximum of ΔC_6^σ increases, reaching its maximal

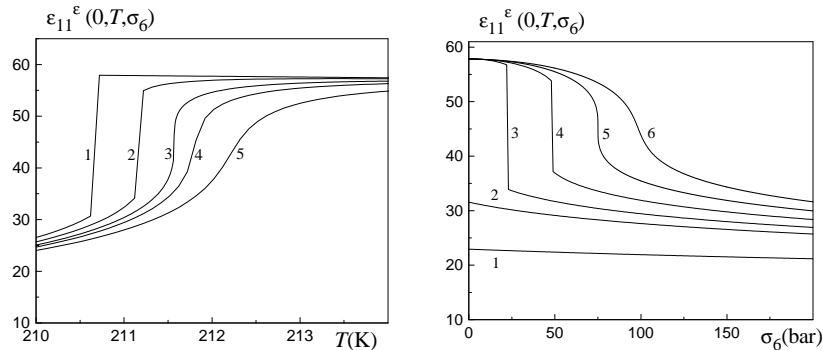


Figure 21. Dependences of dielectric permittivity ε_{11}^e on temperature at different values of stress σ_6 (bar) (left): 1 - 0; 2 - 40; 3 - $\sigma_6^* = 75$; 4 - 100; 5 - 150 and on stress σ_6 at different values of temperature T (K) (right): 1 - 209.0; 2 - $T_{C0} = 210.7$; 3 - 211; 4 - 211.3; 5 - $T^* = 211.57$; 6 - 211.8.

value at $\sigma_6 = \sigma_6^*$, whereas the further increase in stress lowers down the maximal value of ΔC_6^σ and shifts it to higher temperatures. Under stress σ_6 the jump ΔC_6^σ is smeared out.

At temperatures lower than T_C , the ΔC_6^σ increases with stress σ_6 . At $T < T_C^*$ the magnitude of ΔC_6^σ first slightly increases with stress, and then at stresses corresponding to the curve of phase equilibrium it exhibits a sharp increase, diverging at $T = T_C^*$ and $\sigma_6 = \sigma_6^*$ ΔC_6^σ . The further increase in stress gradually decreases ΔC_6^σ . At temperatures $T > T_C^*$, the specific heat ΔC_6^σ smoothly increases with stress, reaches a maximum and smoothly decreases.

Temperature and stress dependences of the pyroelectric coefficient p_6^σ and of the coefficient of linear expansion α_6 are analogous to those of the specific heat ΔC_6^σ .

6. Concluding remarks

In this paper we present the microscopic model for a description of the stress σ_6 on the phase transition, static dielectric, elastic, piezoelectric, and thermal properties of deuterated ferroelectrics of the KD_2PO_4 -type. Unlike hydrostatic or uniaxial $p = -\sigma_3$ pressures, the stress σ_6 lowers the symmetry of the high-temperature phase down to the symmetry of the low-temperature phase. As the electric field E_3 , the stress σ_6 induces in

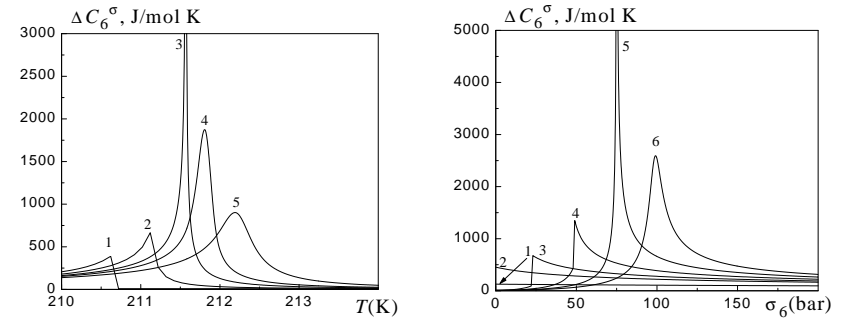


Figure 22. Dependences of specific heat ΔC_6^σ on temperature at different values of stress σ_6 (bar) (left): 1 - 0; 2 - 40; 3 - $\sigma_6^* = 75$; 4 - 100; 5 - 150 and on stress σ_6 at different values of temperature T (K) (right): 1 - 209.0; 2 - $T_{C0} = 210.7$; 3 - 211; 4 - 211.3; 5 - $T^* = 211.57$; 6 - 211.8.

KD_2PO_4 -type crystals the strain ε_6 and, due to the piezoelectric effect, polarization P_3 .

In our previous papers we showed that an important role in dependences of the transition temperature and dielectric characteristics of hydrogen bonded crystals of the KH_2PO_4 -family on pressures that do not change the system symmetry is played by the corresponding changes in hydrogen bond geometry, in particular, in the distance δ between possible deuteron sites on a bond. Most likely, the stress σ_6 does not perceptibly affects δ . Instead, it alters the angle between hydrogen bonds, perpendicular in an unstrained paraelectric crystal, splitting thereby energies of deuteron configurations. Another important mechanism of the stress σ_6 influence on the phase transition and physical properties of the KD_2PO_4 -type ferroelectrics is the piezoelectric coupling, giving rise to effective fields, action of which, for the symmetry reasons, is equivalent to action of an external electric field applied along the ferroelectric axis.

As we show, the transition temperature increases with the stress σ_6 , and the order of the phase transition tends to the second one. In the constructed phase diagram, which has the same topology as the predicted in the phenomenologic approach $T_C - E_3$ diagram, there are two symmetric critical points where the second order phase transitions take place, and the curves of phase equilibrium terminate. The stresses above critical smear off the phase transition and smoothen the temperature dependences of polarization and strain. Correspondingly, an increase in

the stress σ_6 raises up the peak values of the physical characteristics of a crystal having peculiarities in the transition point (the longitudinal dielectric permittivity, compliance s_{66}^E , piezomodules d_{36} and e_{36} , and the specific heat). These peak values are the highest at critical stresses, the higher stresses smoothen the temperature dependences of these characteristics and lower down the peaks.

Taking into account the piezoelectric effect in the developed model allows one, at the proper choice of the theory parameters, to quantitatively describe the available experimental data for the temperature dependences of dielectric, elastic, piezoelectric, and thermal characteristics of unstrained KD_2PO_4 . Further experimental studies are required to ascertain the values of the theory parameters and verify its predictions about the form of the $T_C - \sigma_6$ phase diagram and possible stress σ_6 effects on the physical characteristics of the crystals.

Acknowledgements

This work was supported by the Foundation for Fundamental Investigations of the Ukrainian Ministry in Affairs of Science and Technology, project No 2.04/171.

References

1. Stasyuk I.V., Biletskii I.N. Influence of omnidirectional and uniaxial stress on the ferroelectric phase transition in crystals of KH_2PO_4 type. // Bull. Ac. Sci. USSR, Phys. Ser., 1983, vol. 4, No 4, p. 79-82.
2. Stasyuk I.V., Biletskii I.N., Styahar O.N. Pressure induced phase transitions in KD_2PO_4 crystals. // Ukr. Fiz. Journ., 1986, vol.31, No 4, p. 567-571. (in Russian)
3. Stasyuk I.V., Biletsky I.N. The phase transition in the uniaxially strained ferroelectrics of KD_2PO_4 -type. / Preprint ITF-83-93P. (in Russian)
4. Stasyuk I.V., Zachek I.R., Levitskii R.R., Kukushkin K.V. Influence of the Uniaxial Stress $\sigma_{xx} - \sigma_{yy}$ on the Phase Transition and Thermodynamic Properties of the KD_2PO_4 -Type Hydrogen Bonded Ferroelectrics. / Preprint, ICMP-93-11E, Kyiv, 1993, 37 p.
5. Stasyuk I.V., Levitskii R.R., Zachek I.R., Krokhmal'ski T.Ye., Duda A.S. Uniaxial pressure $\sigma_1 - \sigma_2$ influence on phase transition and physical properties of the KD_2PO_4 -type hydrogen bonded ferroelectrics. // Preprint, ICMP-97-11E, Lviv, 1997, 22 p.

6. Stasyuk I.V., Levitskii R.R., Moina A.P. External pressure influence on ferroelectrics and antiferroelectrics of the KH_2PO_4 family: A unified approach. // Phys. Rev. B., 1999, vol. 59, p. 8530-8540.
7. Stasyuk I.V., Levitskii R.R., Zachek I.R., Moina A.P., Duda A.S. Hydrostatic pressure influence on phase transition and physical properties of KD_2PO_4 -type ferroelectrics. // Cond. Matt. Phys., 1996, No 8, p. 129-156.
8. Stasyuk I.V., Levitskii R.R., Zachek I.R., Duda A.S., Moina A.P., Romanyuk N.O., Stadnyk V.I., Chervony R.G., Shcherbina Ye.V. Uniaxial pressure influence on phase transition and physical properties of highly deuterated $\text{K}(\text{H}_{1-x}\text{D}_x)_2\text{PO}_4$ -type ferroelectrics. // Preprint, ICMP-96-18E, Lviv, 1996, 36 p.
9. Glauber R.J. Time-dependent statistics of the Ising model. // J. Math. Phys., 1963, v. 4, N 2, p. 294-307.
10. Yomosa S., Nagamija T. The Phase Transition and the Piezoelectric Effect of KH_2PO_4 . // Progr. Ther. Phys., 1949, v. 4, N 3, p. 263-274.
11. R. Blinc and B. Žekš, *Soft modes in ferroelectrics and antiferroelectrics* (Elseviers, New York, 1974).
12. R. Blinc and B. Žekš, *Helv. Phys. Acta* **41**, 701 (1968).
13. N.I.Stadnik, N.A.Romanyuk, and R.G. Chervonyj, *Opt. Spectrosk.* **84**, 273 (1998).
14. V.G. Vaks, N.E. Zein, and Strukov B.A, *Phys. Status Solidi A* **30**, 801 (1975).
15. W.P.Mason. *Physical acoustics and properties of solids*.
16. Bantle W., Caffish C. *Helv. Phys. Acta*, 1943, vol. 16, p. 235.
17. Von Arx A., Bantle W. *Helv. Phys. Acta*, 1943, vol. 16, p. 211.
18. Brody E.M., Cummins H.Z. *Phys. Rev. Lett.*, 1968, vol. 21, p. 1263.
19. L.A.Shuvalov, I.S. Zheludev et al. Ferroelectric anomalies of dielectric and piezoelectric properties of RbH_2PO_4 and KD_2PO_4 crystals. // Bull. Ac. Sci. USSR, Ser. Fiz., 1967, vol. 31, No 11, p. 1919-1922. (in Russian)
20. Shuvalov L.A., Mnatsakanyan A.V. The elastic properties of KD_2PO_4 crystals over a wide temperature range. // *Sov. Phys. Crystall.*, 1966, vol. 11, №2, p. 210-212.
21. I.V.Stasyuk, R.R.Levytsky, N.A.Korinevskii. Collective vibrations of protons in compounds of KH_2PO_4 -type. The cluster approximation. // *phys. stat. sol. (b)*, 1979, col.91, No 2, p. 541-550.
22. Levitskii R.R., Stasyuk I.V., Korinevskii N.A. Dynamics of ferroactive crystals of orthophosphate type. // *Ferroelectrics*, 1978, vol. 21, p.481-483.
23. Blinc R, Schmidt V.H. Soft modes and proton tunneling in PbHPO_4 ,

- squaric acid and KH_2PO_4 type ferroelectrics. // *Ferroelectrics Letters*, 1984, vol. 1, p.119-129.
24. R.R. Levitskii, I.R. Zachek, and I.Ye. Mits, Thermodynamics and longitudinal relaxation of $\text{K}(\text{H}_{1-x}\text{D}_x)_2\text{PO}_4$ ferroelectrics. / Preprint Inst. Theor. Phys., ITP-87-114R, 1987 (in Russian).
 25. R.R. Levitskii, I.R. Zachek, and I.Ye. Mits. Transverse relaxation in $\text{K}(\text{H}_{1-x}\text{D}_x)_2\text{PO}_4$ type ferroelectrics. Preprint Inst. Theor. Phys., ITP-87-115R, 1987 (in Russian).
 26. Devonshire A.F. Theory of ferroelectrics. // *Adv. Phys.*, 1954, vol. 3, No 10, p. 85-130.
 27. A. Western, A.G.Baker, C.P.Bacon, V.H.Schmidt. Pressure-induced tricritical point in the ferroelectric phase transition of KH_2PO_4 . // *Phys. Rev. B*, 1978, vol. 17, p. 4461-4473.
 28. Merz W.J. Double hysteresis loop of BaTiO_3 at the Curie point. // *Phys. Rev.*, 1953, vol. 91, No 3, p. 513-517.
 29. V.V.Gladkii, E.V. Sidnenko. Double loops of the dielectric hysteresis in KD_2PO_4 crystal. // *Sov. Phys. Solid State*, 1972, vol. 13, p. 2592.
 30. Baumgartner H. // *Helv. Phys. Acta*, 1950, vol. 23, p. 651.

Препринти Інституту фізики конденсованих систем НАН України розповсюджуються серед наукових та інформаційних установ. Вони також доступні по електронній комп'ютерній мережі на WWW-сервері інституту за адресою <http://www.icmp.lviv.ua/>

The preprints of the Institute for Condensed Matter Physics of the National Academy of Sciences of Ukraine are distributed to scientific and informational institutions. They also are available by computer network from Institute's WWW server (<http://www.icmp.lviv.ua/>)

Ігор Васильович Стасюк
Роман Романович Левицький
Ігор Романович Зачек
Алла Пилипівна Моїна
Андрій Степанович Дуда

ВПЛИВ НАПРУГИ ЗСУВУ σ_6 НА ФАЗОВИЙ ПЕРЕХІД І ФІЗИЧНІ
ВЛАСТИВОСТІ СЕГНЕТОЕЛЕКТРИКІВ ТИПУ KD_2PO_4

Роботу отримано 17 грудня 1999 р.

Затверджено до друку Вченою радою ІФКС НАН України

Рекомендовано до друку семінаром відділу теорії модельних
спінових систем

Виготовлено при ІФКС НАН України

© Усі права застережені